

We are IntechOpen, the world's leading publisher of Open Access books Built by scientists, for scientists

6,900

Open access books available

186,000

International authors and editors

200M

Downloads

Our authors are among the

154

Countries delivered to

TOP 1%

most cited scientists

12.2%

Contributors from top 500 universities



WEB OF SCIENCE™

Selection of our books indexed in the Book Citation Index
in Web of Science™ Core Collection (BKCI)

Interested in publishing with us?
Contact book.department@intechopen.com

Numbers displayed above are based on latest data collected.
For more information visit www.intechopen.com



From Conditional Probability Measurements to Global Matrix Representations on Variant Construction – A Particle Model of Intrinsic Quantum Waves for Double Path Experiments

Jeffrey Zheng¹, Christian Zheng² and T.L. Kunii³

¹*Yunnan University*

²*University of Melbourne*

³*University of Tokyo*

¹*P.R. China*

²*Australia*

³*Japan*

1. Introduction

1.1 Two types of double slit experiments

Quantum statistics play a key role in Quantum Mechanics QM [Feynman et al. (1965,1989); Penrose (2004)]. Two types of Double Slit Experiment are used to explore the core mysteries of quantum interactive behaviors. These are standard Double Slit Experiments with correlated signals and Single Photon Experiments that use ultra low intensity and lengthy exposures to demonstrate quanta self-interference patterns. The key significance is that intrinsic wave properties are observed in both environments [Barrow et al. (2004); Hawking and Mlodinow (2010)].

1.2 Two types of probabilities

Multivariate probabilities acting on multinomial distributions occupy a central role in classical probability theory and its applications. This mechanism has been explored from the early days in the study of modern probability theories [Ash & Doléans-Dade (2000); Durrett (2005)]. Conditional probability is a powerful methodology at the heart of classical Bayesian statistics. In the history of probability and statistical developments, there have been long-running debates and a persistent lack of agreement in differentiating between prior distributions and posterior distributions [Ash & Doléans-Dade (2000); Durrett (2005)]. It is worthy of note that the uniform distributions or normal distributions of conditional probability are always linked to a relatively large number of probability distributions in non-normal conditions. This points to practical problems with random distributions.

1.3 Advanced single photon experiments

1.3.1 Applying the bohr complementarity principle

The Bohr Complementarity Principle BCP, established back in the 1920s brought us the foundations of QM [Bohr (1949)]. In Bohr's statement: "... we are presented with a choice of either tracing the path of the particle; or observing interference effects ... we have here to do with a typical example of how the complementary phenomena appear under mutually exclusive experimental arrangements." It is significant that BCP provided a powerful intellectual basis for Bohr in key debates in the history of QM and especially in his debates with Einstein [Jammer (1974)].

1.3.2 Testing bell inequality

To help decide between Bohr and Einstein on their approaches to wave and particle issues, Bell proposed a set of Bell-Inequations in the 1960s [Bell (1964)]. In 1969, CHSH proposed a spin measurement approach [Clauser et al. (1969)] and experiments by Aspect in 1982 did not support local realism [Aspect et al. (1982)].

1.3.3 Afshar's measurements

In 2001 Afshar set up an experiment to test the BCP [Afshar (2005)]. This experiment generated strong evidence contradicting the BCP, since both particle and wave distributions can be observed simultaneously. In Afshar's experiments, there are four measurements: ψ_1 - signals via left path, ψ_2 - signals via right path, σ_1 - interactive measurements of $\{\psi_1, \psi_2\}$ on the distance of f , and σ_2 - separate measurements of $\{\psi_1, \psi_2\}$ on the distance of $f + d$ respectively. In this experiment, a measurement quaternion is

$$\langle \psi_1, \psi_2, \sigma_1, \sigma_2 \rangle. \quad (1)$$

1.4 Current situation

From the 1920s through to the start of the 21st century, there was no significant experimental evidence to show that there were problems with the BCP. However, Afshar's 2001 experimental results are clearly not consistent with the BCP and further experimental results have provided solid evidence against the BCP. [Afshar (2005; 2006); Afshar et al. (2007)]. It is interesting to see that neither local realism nor the BCP are validated by the results of modern advanced single photon experiments [Afshar et al. (2007); Aspect (2007)]. It will be a major challenge in this century to redefine the principles on which the quantum approach may now be safely founded.

1.5 Chapter organization

Following on from multivariate probability models, this chapter focusses on a conditional approach to illustrate special properties found in conditional probability measurements via global matrix representations on the variant construction. This chapter is organized into nine sections addressing as follows:

1. general introduction (above)
2. key historical debates on the foundations of QM

3. analysis of key issues of QM
4. conditional construction proposed
5. exemplar results
6. analysis of visual distributions
7. using the variant solution to resolve longstanding puzzles
8. main results
9. final conclusions

2. Wave and particle debates in QM developments

2.1 Heisenberg uncertain principle

The Heisenberg Uncertainty Principle HUP was established in 1927 [Heisenberg (1930)]. The HUP represented a milestone in the early development of quantum theory [Jammer (1974)]. It implies that it is impossible to simultaneously measure the present position of a particle while also determining the future motion of a particle or any system small enough to require a Quantum mechanical treatment. From a mathematical viewpoint, the HUP arises from an equation following the methodology of Fourier analysis for the motion $[Q, P] = QP - PQ = i\hbar$. The later form of HUP is expressed as $\Delta p \cdot \Delta q \approx h$.

This equation shows that the non-commutativity implies that the HUP provides a physical interpretation for the non-commutativity.

2.2 Bohr complementarity principle

The HUP provided Bohr with a new insight into quantum behaviors [Bohr (1958)]. Bohr established the BCP to extend the idea of complementary variables for the HUP to energy and time, and also to particle and wave behaviors. One must choose between a particle model, with localized positions, trajectories and quanta or a wave model, with spreading wave functions, delocalization and interferences [Jammer (1974)].

Under the BCP, complementary descriptions e.g. wave or particle are mutually exclusive within the same mathematical framework because each model excludes the other. However, a conceptual construction allowed the HUP, the BCP and wave functions together with observed results to be integrated to form the Copenhagen Interpretation of QM. In the context of double slit experiments, the BCP dictates that the observation of an interference pattern for waves and the acquisition of directional information for particles are mutually exclusive.

2.3 Bohr-Einstein debates on wave and particle issues

Bohr and Einstein remained lifelong friends despite their differences in opinion regarding QM [Bohr (1949; 1958)]. In 1926 Born proposed a probability theory for QM without any causal explanation. Einstein's reaction is well known from his letter to Born [Born (1971)] in which he said "I, at any rate, am convinced that HE [God] does not throw dice."

Then in 1927 at the Solvay Conference, Heisenberg and Bohr announced that the QM revolution was over with nothing further being required. Einstein was dismayed [Bohr (1949); Bolles (2004)] for he believed that the underlying effects were not yet properly understood.

Perhaps in a spirit of compromise, Bohr then proposed his BCP that emphasizes the role of the observer over that which is observed. From 1927-1935, Einstein proposed a series of three intellectual challenges to further explore wave and particle issues [Bohr (1935; 1949); Bolles (2004)]:

- First, in 1927 Einstein proposed a double slit experiment on interference properties.
- Second, in 1930 at the sixth Solvay Congress, Einstein proposed weighing a box emitting timed releases of electromagnetic radiation.
- Third, in 1935 the paper "Can Quantum Mechanical Of Description Physical Reality Be Considered Complete?" [Einstein et al. (1935)] by Einstein, Podolsky and Rosen EPR was published in Physical Review.

2.4 EPR claims

The key points of the EPR paper are focused on two aspects: either (1) the description of reality given by the wave function in QM is incomplete or (2); the two quantities P and Q cannot have simultaneous reality.

Both operations: P and Q are applied $PQ - QP = i\hbar$. Such relationships follow the standard Quantum expression.

Property $PQ - QP \neq 0$ implies P and Q operations are related without independent computational properties. Under this condition, it is impossible to execute the two operations simultaneously under extant QM frameworks. From a parallel processing viewpoint, Einstein's view is extremely valuable. As such modern parallel computing theories and practices were only developed in the 1970s [Valiant (1975)] it is remarkable that Einstein pioneered such an approach way back in the 1930s. Modern parallel computing theory and practice support the original EPR paper and the conclusion that a QM description of physical that is expressed only in terms of wave functions is incomplete.

3. Key issues in QM

3.1 Restriction under HUP

For the HUP, different interpretations originate from the equation $[Q, P] = QP - PQ = i\hbar$, and the later HUP form $\Delta q \cdot \Delta p \geq h$. From a mathematical viewpoint, this type of inequality implies $\Delta q, \Delta p \geq h$ too. In other words, a minimal grid of a lattice restricts Δq and $\Delta p \rightarrow 0$ actions. From the HUP expression, $[Q, P] \neq 0$ indicates the construction with a discrete intrinsic limitation. Such structures cannot directly apply to continuous infinitesimal operations.

Many quantum problems do not extend to the region of Plank constant limitations. Investigation back in the 1930s tended to rely more on theoretical considerations rather than actual experimentation [Bohr (1949)]. Consequently many issues had to wait until the 1980s to become better understood.

Both Q and P are infinite dimensional matrices, the restriction of $[Q, P] = i\hbar$ comes with a clear meaning today on its discrete properties. We cannot apply a continuous approach to make $[Q, P] = 0$. From an operational viewpoint, Einstein correctly identified the root of the matter. Since Q and P cannot exchange, it is not possible to run a simultaneous process on the

standard wave functions. Simply extending discrete variations using continuous approaches presents further difficulties for the HUP.

In addition, the following questions need to be addressed in relation to the practical identification of complementary objects.

- What determines when a pair of objects is indeed a complementary pair?
- Is a pair of complex conjugate objects: $a + bi$ and $a - bi$, a pair of complementary objects?
- Is a pair of matrices, a hermit matrix H and its complex conjugate matrix H^* , a pair of complementary objects?
- Why can density matrix operations on infinite dimension be performed without significant errors while a pair of complementary finite matrices must be restricted by the HUP?

In practice, QM computations are mainly applied to wave functions and $[Q, P] = i\hbar$ formula. Intellectual debate on the theoretical considerations is particularly relevant to the HUP. In comparison, the deeper problems of QM cannot be easily explored in the absence of an experimental approach and a viable alternative theoretical construction [Barrow et al. (2004); Jammer (1974)].

3.2 Construction of BCP

Inspired by the HUP, Bohr uses a continuous analogy and a classical logical construction to describe Quantum systems. The BCP extends the HUP to handle different pairs of opposites and to restrict them with exclusive properties [Bohr (1958)].

As there were no well refined critical experiments in these days, all the debates between Bohr and Einstein were based on theoretical considerations alone. Compared with Einstein's open-minded attitudes to QM [Einstein et al. (1935)], Bohr and others insisted on the completeness and consistency of the Copenhagen Interpretation on QM [Bohr (1935)]. Such closed attitudes served to distance Bohr and others of like mind from reasonable suggestions made by Einstein and those expressed in the EPR paper and to lead them to treat such suggestions as if they were attacks on their already strongly held views [Bolles (2004)].

The BCP uses a classical logic framework to support dynamic constructions. Underpinned by the BCP, the HUP and a knowledge of wave functions, the Copenhagen Interpretation played a dominant role in QM from the 1930s on as it had by then been accepted as the orthodox point of view [Jammer (1974)].

Meanwhile, the EPR paper emphasizes that critical evidence must be obtained by real experiments and measurements. It is in the nature of a priori philosophical considerations that they will run into difficulties when actual experimental results fail to corresponded with their expectations.

3.3 EPR construction

The EPR position [Einstein et al. (1935)] can be re-visited in the light of modern advances in knowledge and computing theory. From a computing viewpoint, simultaneous properties may be the key with which these long-standing mysteries of QM can at last be unlocked. Operators P and Q cannot be exchanged, this indicates operational relevances existing in the lower levels of classical QM construction. In addition, there is a requirement of two systems

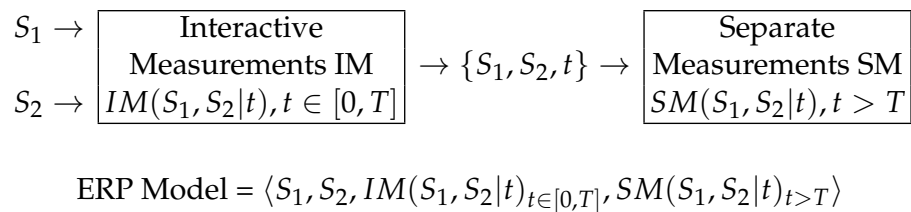


Fig. 1. EPR Measurement Quaternion Model on Einstein's Experimental Devices

to have interactive properties in $t \in [0, T]$ and without interactive properties on $t > T$. Such expressions may not be properly formulated by Fourier transformation schemes on wave functions.

However, after 78 years of development in advanced scientific and ICT technologies, it is now possible to use advanced photonic and optical fiber technologies to implement all the requirements of the experiments proposed by Einstein.

The core EPR model can be shown in Figure 1, listed notations are explained as follows.

Let S_1 be System I, S_2 be System II, $IM(S_1, S_2|t), t \in [0, T]$ be Interactive Measurements IM for S_1 and S_2 on $t \in [0, T]$, $SM(S_1, S_2|t), t > T$ be Separate Measurements SM (non-interactive measurements) for S_1 and S_2 on $t > T$. Einstein's Experimental devices can be described as an EPR measurement quaternion:

$$\langle S_1, S_2, IM(S_1, S_2|t)_{t \in [0, T]}, SM(S_1, S_2|t)_{t > T} \rangle. \quad (2)$$

If an experiment can be expressed in the requisite form for this model, then it can be legitimately claimed as an EPR experiment.

3.4 Afshar experimental device

Afshar's experimental results have shown that it is possible to measure both particle and wave interference properties simultaneously in the same experiment with high accuracy [Afshar (2005; 2006); Afshar et al. (2007)]. Since this set of experiments has produced results that challenge the BCP at its very core it is pertinent to analyze and compare the model with the requirements for valid EPR devices.

In Afshar's experiments, $\{\psi_1, \psi_2\}$ are two signals input through double slits; σ_1 is the location on the distance f to collect interference measurements of $\{\psi_1, \psi_2\}$, and σ_2 is the location on the distance $f + d$ to collect separate measurements of $\{\psi_1, \psi_2\}$. Under this configuration, a 1-1 corresponding map can be established as follows:

$$\left\{ \begin{array}{l}
 \psi_1 \rightarrow S_1; \\
 \psi_2 \rightarrow S_2; \\
 \sigma_1 \rightarrow IM(S_1, S_2|t), t \rightarrow f; \\
 \sigma_2 \rightarrow SM(S_1, S_2|t), t \rightarrow f + d.
 \end{array} \right. \quad (3)$$

Using quaternion structures,

$$\langle \psi_1, \psi_2, \sigma_1, \sigma_2 \rangle \rightarrow \langle S_1, S_2, IM(S_1, S_2|f), SM(S_1, S_2|f + d) \rangle. \quad (4)$$

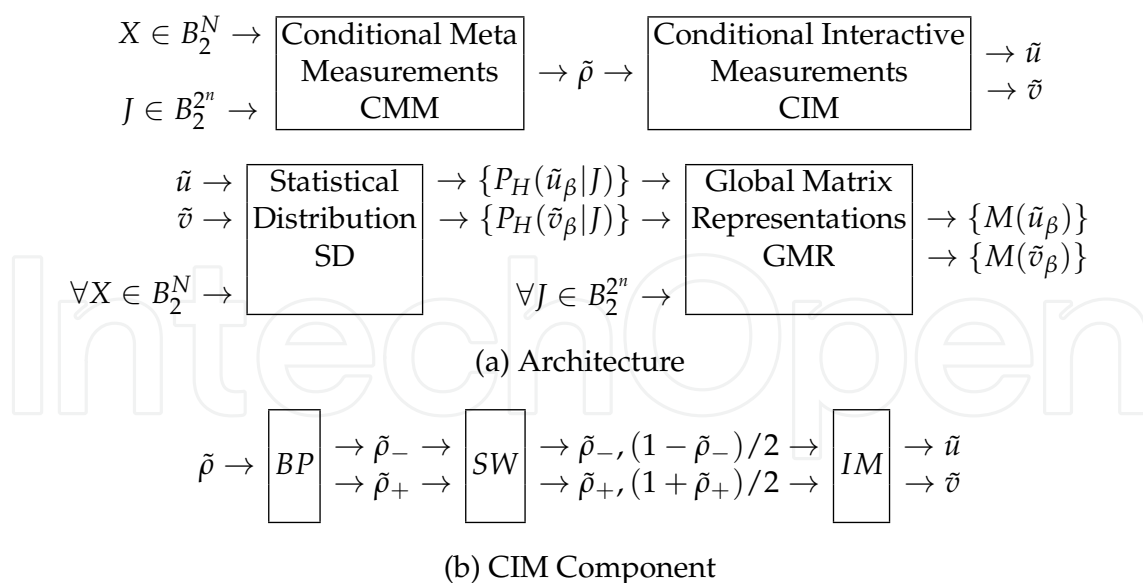


Fig. 2. (a-b) Conditional Variant Simulation and Representation System; (a) System Architecture; (b) Conditional Interactive Measurement CIM Component

Under this correspondence, Afshar experiments are consistent with the EPR model.

4. Conditional variant simulation and representation system

A comprehensive review of the process of variant construction from conditional probability measurements through to global matrix representations is described briefly in this section. It is hoped that this may offer a convenient path for those seeking to devise and carry out experiments to further explore natural mysteries through the application of sound principles of logic and measurement.

Using variant principles described in the following subsections, with a N bit 0-1 vector X and a given logic function f , all N bit vectors are exhausted, variant measures generate two groups of histograms. The variant simulation and representation system is shown in Fig 2 (a-b). The detailed principles and methods are described in Sections 4.2-4.7 respectively. For multivariate probability conditions, please refer to the chapter of "From local interactive measurements to global matrix representations on variant construction" elsewhere in this book for sample cases and group distributions in multivariate probability environments.

4.1 Conditional simulation and representation model

The full measurement and representational architecture as shown in Figure 2(a) has four components: Conditional Meta Measurements CMM, Conditional Interactive Measurements CIM, Statistical Distributions SD and Global Matrix Representations GMR. The key part of the system, the CIM component, is shown in Fig 2(b).

4.1.1 Conditional Meta Measurements

The Conditional Meta Measurement (CMM) component uses N bit 0-1 vector X and a given function $J \in B_2^{2^n}$, CMM transfers N bit 0-1 vector under $J(X)$ to generate four Meta-measures,

under a given probability scheme, four conditional probability measurements are generated and output as a quaternion signal $\tilde{\rho}$.

4.1.2 Conditional Interactive Measurements

The Conditional Interactive Measurement (CIM) component is the key location for conditional interactions as shown in Figure 2(b) to transfer a quaternion signal $\tilde{\rho}$ under symmetry / anti-symmetry and synchronous / asynchronous conditions, under four combinations of time effects namely (Left, Right, Double Particle, Double Wave). Two types of additive operations are identified. Each $\{\tilde{u}, \tilde{v}\}$ signal is composed of four distinct signals.

4.1.3 Statistical Distributions

The Statistical Distribution (SD) component performs statistical activities on corresponding signals. It is necessary to exhaust all possible vectors of X with a total of 2^N vectors. Under this construction, each sub-signal of $\{\tilde{u}, \tilde{v}\}$ forms a special histogram with a one dimensional spectrum to indicate the distribution under function J . A total of eight histograms are generated in the probability conditions.

4.1.4 Global Matrix Representations

The Global Matrix Representation (GMR) component uses each statistical distribution of the relevant probability histogram as an element of a matrix composed of a total of 2^{2^n} elements for all possible functions $\{J\}$. In this configuration, C code schemes are applied to form a $2^{2^{n-1}} \times 2^{2^{n-1}}$ matrix to show the selected distribution group.

Unlike the other coding schemes (SL, W, F, ...), only C code schemes provide a regular configuration to clearly differentiate the Left path as exhibiting horizontal actions and the Right path as exhibiting vertical actions. Such clearly polarized outcomes may have the potential to help in the understanding of interactive mechanism(s) between double path for particles and double path for waves properties.

4.2 Variant principle

The variant principle is based on n -variable logic functions [Zheng (2011); Zheng & Zheng (2010; 2011a;b); Zheng et al. (2011)].

4.2.1 Two sets of states

For any n -variables $x = x_{n-1} \dots x_i \dots x_0$, $0 \leq i < n$, $x_i \in \{0, 1\} = B_2$ let a position j be the selected bit $0 \leq j < n$, x_j be the selected variable. Let output variable y and n -variable function f , $y = f(x)$, $y \in B_2$, $x \in B_2^n$. For all states of x , a set $S(n)$ composed of the 2^n states can be divided into two sets: $S_0(n)$ and $S_1(n)$.

$$\begin{cases} S_0(n) = \{x | x_j = 0, \forall x \in B_2^n\} \\ S_1(n) = \{x | x_j = 1, \forall x \in B_2^n\} \\ S(n) = \{S_0(n), S_1(n)\} \end{cases} \quad (5)$$

4.2.2 Four meta functions

For a given logic function f , input and output pair relationships define four meta logic functions $\{f_{\perp}, f_{+}, f_{-}, f_{\top}\}$.

$$\begin{cases} f_{\perp}(x) = \{f(x)|x \in S_0(n), y = 0\} \\ f_{+}(x) = \{f(x)|x \in S_0(n), y = 1\} \\ f_{-}(x) = \{f(x)|x \in S_1(n), y = 0\} \\ f_{\top}(x) = \{f(x)|x \in S_1(n), y = 1\} \end{cases} \quad (6)$$

4.2.3 Two polarized functions

Considering two standard logic canonical expressions: the AND-OR form is selected from $\{f_{+}(x), f_{\top}(x)\}$ as $y = 1$ items, and the OR-AND form is selected from $\{f_{-}(x), f_{\perp}(x)\}$ as $y = 0$ items. Considering $\{f_{\top}(x), f_{\perp}(x)\}$, $x_j = y$ items, they are themselves invariant.

To select $\{f_{+}(x), f_{-}(x)\}$, $x_j \neq y$ in forming a variant logic expression. Let $f(x) = \langle f_{+}|x|f_{-} \rangle$ be a variant logic expression. Any logic function can be expressed as a variant logic form. In $\langle f_{+}|x|f_{-} \rangle$ structure, f_{+} selected 1 items in $S_0(n)$ as the same as the AND-OR standard expression, and f_{-} selecting relevant parts the same as OR-AND expression 0 items in $S_1(n)$.

4.3 Meta measures and conditional probability measurements

Under variant construction, N bits of 0-1 vector X under a function J produce four Meta measures composed of a measure vector N

$$(X : J(X)) \rightarrow (N_{\perp}, N_{+}, N_{-}, N_{\top}), N_0 = N_{\perp} + N_{+}, N_1 = N_{-} + N_{\top}, N = N_0 + N_1$$

Using four Meta measures, relevant probability measurements can be formulated.

$$\tilde{\rho} = (\tilde{\rho}_{\perp}, \tilde{\rho}_{+}, \tilde{\rho}_{-}, \tilde{\rho}_{\top}) = (N_{\perp}/N_0, N_{+}/N_0, N_{-}/N_1, N_{\top}/N_1), 0 \leq \tilde{\rho}_{\perp}, \tilde{\rho}_{+}, \tilde{\rho}_{-}, \tilde{\rho}_{\top} \leq 1.$$

4.3.1 Variant measure functions

Let Δ be the variant measure function

$$\begin{aligned} \Delta &= \langle \Delta_{\perp}, \Delta_{+}, \Delta_{-}, \Delta_{\top} \rangle \\ \Delta J(x) &= \langle \Delta_{\perp} J(x), \Delta_{+} J(x), \Delta_{-} J(x), \Delta_{\top} J(x) \rangle \\ \Delta_{\alpha} J(x) &= \begin{cases} 1, & J(x) \in J_{\alpha}(x), \alpha \in \{\perp, +, -, \top\} \\ 0, & \text{others} \end{cases} \end{aligned} \quad (7)$$

For any given n -variable state there is one position in $\Delta J(x)$ to be 1 and other 3 positions are 0.

4.3.2 Variant measures on vector

For any N bit 0-1 vector X , $X = X_{N-1} \dots X_j \dots X_0$, $0 \leq j < N$, $X_j \in B_2$, $X \in B_2^N$ under n -variable function J , n bit 0-1 output vector Y , $Y = J(X) = \langle J_{+}|X|J_{-} \rangle$, $Y = Y_{N-1} \dots Y_j \dots Y_0$, $0 \leq j < N$, $Y_j \in B_2$, $Y \in B_2^N$. For the j -th position $x^j = [\dots X_j \dots] \in B_2^n$ to form $Y_j = J(x^j) = \langle J_{+}|x^j|J_{-} \rangle$.

Let N bit positions be cyclic linked. Variant measures of $J(X)$ can be decomposed

$$\Delta(X : Y) = \Delta J(X) = \sum_{j=0}^{N-1} \Delta J(x^j) = \langle N_{\perp}, N_{+}, N_{-}, N_{\top} \rangle \quad (8)$$

as a quaternion $\langle N_{\perp}, N_{+}, N_{-}, N_{\top} \rangle$, $N = N_{\perp} + N_{+} + N_{-} + N_{\top}$.

4.3.3 Example

E.g. $N = 12$, given $J, Y = J(X)$.

$$\begin{aligned} X &= 1 \ 0 \ 1 \ 1 \ 1 \ 0 \ 1 \ 1 \ 1 \ 0 \ 0 \ 1 \\ Y &= 0 \ 0 \ 1 \ 0 \ 1 \ 0 \ 1 \ 0 \ 1 \ 1 \ 0 \ 0 \\ \Delta(X : Y) &= - \ \perp \ \top \ - \ \top \ \perp \ \top \ - \ \top \ + \ \perp \ - \end{aligned}$$

$$\Delta J(X) = \langle N_{\perp}, N_{+}, N_{-}, N_{\top} \rangle = \langle 3, 1, 4, 4 \rangle, N = 12.$$

Input and output pairs are 0-1 variables for only four combinations. For any given function J , the quantitative relationship of $\{\perp, +, -, \top\}$ is directly derived from the input/output sequences. Four meta measures are determined.

4.4 Four conditional meta measurements

Using variant quaternion, conditional measurements of probability signals are calculated as four meta conditional measurements by following the given equations. For any N bit 0-1 vector X , function J , under Δ measurement: $\Delta J(X) = \langle N_{\perp}, N_{+}, N_{-}, N_{\top} \rangle$, $N_0 = N_{\perp} + N_{+}$, $N_1 = N_{-} + N_{\top}$, $N = N_0 + N_1 = N_{\perp} + N_{+} + N_{-} + N_{\top}$.

Signal $\tilde{\rho}$ is defined by

$$\begin{cases} \tilde{\rho} = (\tilde{\rho}_{\perp}, \tilde{\rho}_{+}, \tilde{\rho}_{-}, \tilde{\rho}_{\top}) \\ \tilde{\rho}_{\perp} = \frac{N_{\perp}}{N_0} \\ \tilde{\rho}_{+} = \frac{N_{+}}{N_0} \\ \tilde{\rho}_{-} = \frac{N_{-}}{N_1} \\ \tilde{\rho}_{\top} = \frac{N_{\top}}{N_1} \end{cases} \quad (9)$$

4.5 Conditional Interactive Measurements

Conditional Interactive Measurements (CIM) are divided into three stages: BP, SW and SM respectively. The BP stage selects $\{\tilde{\rho}_{-}, \tilde{\rho}_{+}\}$ as sub-signals. The SW component extends two signals into four signals with different symmetric properties; The SM component merges different signals to form two sets of eight signals.

Using $\{\tilde{\rho}_{+}, \tilde{\rho}_{-}\}$, a pair of signals $\{\tilde{u}, \tilde{v}\}$ are formulated:

$$\begin{cases} \tilde{u} = (\tilde{u}_{+}, \tilde{u}_{-}, \tilde{u}_0, \tilde{u}_1) = \{u_{\beta}\} \\ \tilde{v} = (\tilde{v}_{+}, \tilde{v}_{-}, \tilde{v}_0, \tilde{v}_1) = \{v_{\beta}\} \\ \beta \in \{+, -, 0, 1\} \end{cases} \quad (10)$$

$$\begin{cases} \tilde{u}_+ = \tilde{\rho}_+ \\ \tilde{u}_- = \tilde{\rho}_- \\ \tilde{u}_0 = \tilde{u}_+ \oplus \tilde{u}_- \\ \tilde{u}_1 = (\tilde{u}_+ + \tilde{u}_-)/2 \\ \tilde{v}_+ = \frac{1+\tilde{\rho}_+}{2} \\ \tilde{v}_- = \frac{1-\tilde{\rho}_-}{2} \\ \tilde{v}_0 = \tilde{v}_+ \oplus \tilde{v}_- \\ \tilde{v}_1 = \tilde{v}_+ + \tilde{v}_- - 0.5 \end{cases} \quad (11)$$

where $0 \leq \tilde{u}_\beta, \tilde{v}_\beta \leq 1, \beta \in \{+, -, 0, 1\}, \oplus$: Asynchronous addition, $+$: Synchronous addition.

4.6 Statistical distributions

The SD component provides a statistical means to accumulate all possible vectors of N bits for a selected signal and generate a histogram. Eight signals correspond to eight histograms respectively. Among these, four histograms exhibit properties of symmetry and the other four histograms exhibit properties of anti-symmetry.

4.6.1 Statistical histograms

For a function J , all measurement signals are collected and the relevant histogram represents a complete statistical distribution.

Using \tilde{u} and \tilde{v} signals, each \tilde{u}_β or \tilde{v}_β determines a fixed position in the relevant histogram to make vector X on a position. After completing 2^N data sequences, eight symmetry/anti-symmetry histograms of $\{H(\tilde{u}_\beta|J)\}, \{H(\tilde{v}_\beta|J)\}$ are generated.

For a function $J, \beta \in \{+, -, 0, 1\}$

$$\begin{cases} H(\tilde{u}_\beta|J) = \sum_{\forall X \in B_2^N} H(\tilde{u}_\beta|J(X)) \\ H(\tilde{v}_\beta|J) = \sum_{\forall X \in B_2^N} H(\tilde{v}_\beta|J(X)), J \in B_2^{2^n} \end{cases} \quad (12)$$

4.6.2 Normalized probability histograms

Let $|H(\dots)|$ denote the total number in the histogram $H(\dots)$, a normalized probability histogram ($P_H(\dots)$) can be expressed as

$$\begin{cases} P_H(\tilde{u}_\beta|J) = \frac{H(\tilde{u}_\beta|J)}{|H(\tilde{u}_\beta|J)|} \\ P_H(\tilde{v}_\beta|J) = \frac{H(\tilde{v}_\beta|J)}{|H(\tilde{v}_\beta|J)|}, J \in B_2^{2^n} \end{cases} \quad (13)$$

Here, all histograms are restricted in $[0, 1]^2$ areas.

Distributions are dependant on the data set as a whole and are not sensitive to varying under special sequences. Under this condition, when the data set has been exhaustively listed, then the same distributions are always linked to the given signal set.

The eight histogram distributions provide invariant spectra to represent properties among different interactive conditions.

4.7 Global Matrix Representations

After local interactive measurements and statistical process are undertaken for a given function J , eight histograms are generated. The Global Matrix Representation GMR component performs its operations into two stages. In the first stage, exhausting all possible functions for $\forall J \in B_2^{2^n}$ to generate eight sets, each set contains 2^{2^n} elements and each element is a histogram. In the second stage, arranging all 2^{2^n} elements generated as a matrix by C code scheme. Here, we can see Left and Right path reactions polarized into Horizontal and Vertical relationships respectively.

4.7.1 Matrix and its elements

For a given C scheme, let $C(J) = \langle J^1 | J^0 \rangle$, each element

$$\begin{cases} M_{\langle J^1 | J^0 \rangle}(\tilde{u}_\beta | J) = P_H(\tilde{u}_\beta | J) \\ M_{\langle J^1 | J^0 \rangle}(\tilde{v}_\beta | J) = P_H(\tilde{v}_\beta | J) \\ J \in B_2^{2^n}; J^1, J^0 \in B_2^{2^{n-1}} \end{cases} \quad (14)$$

4.7.2 Representation patterns of matrices

For example, using $n = 2, P = (3102), \Delta = (1111)$ conditions, a C code case contains sixteen histograms arranged as a 4×4 matrix.

0	4	1	5
2	6	3	7
8	12	9	13
10	14	11	15

(15)

All matrices in this chapter use this configuration for the matrix pattern representing their elements.

5. Simulation results

For ease of illustration, as different signals have intrinsic random properties, only statistical distributions and global matrix representations are selected in this section.

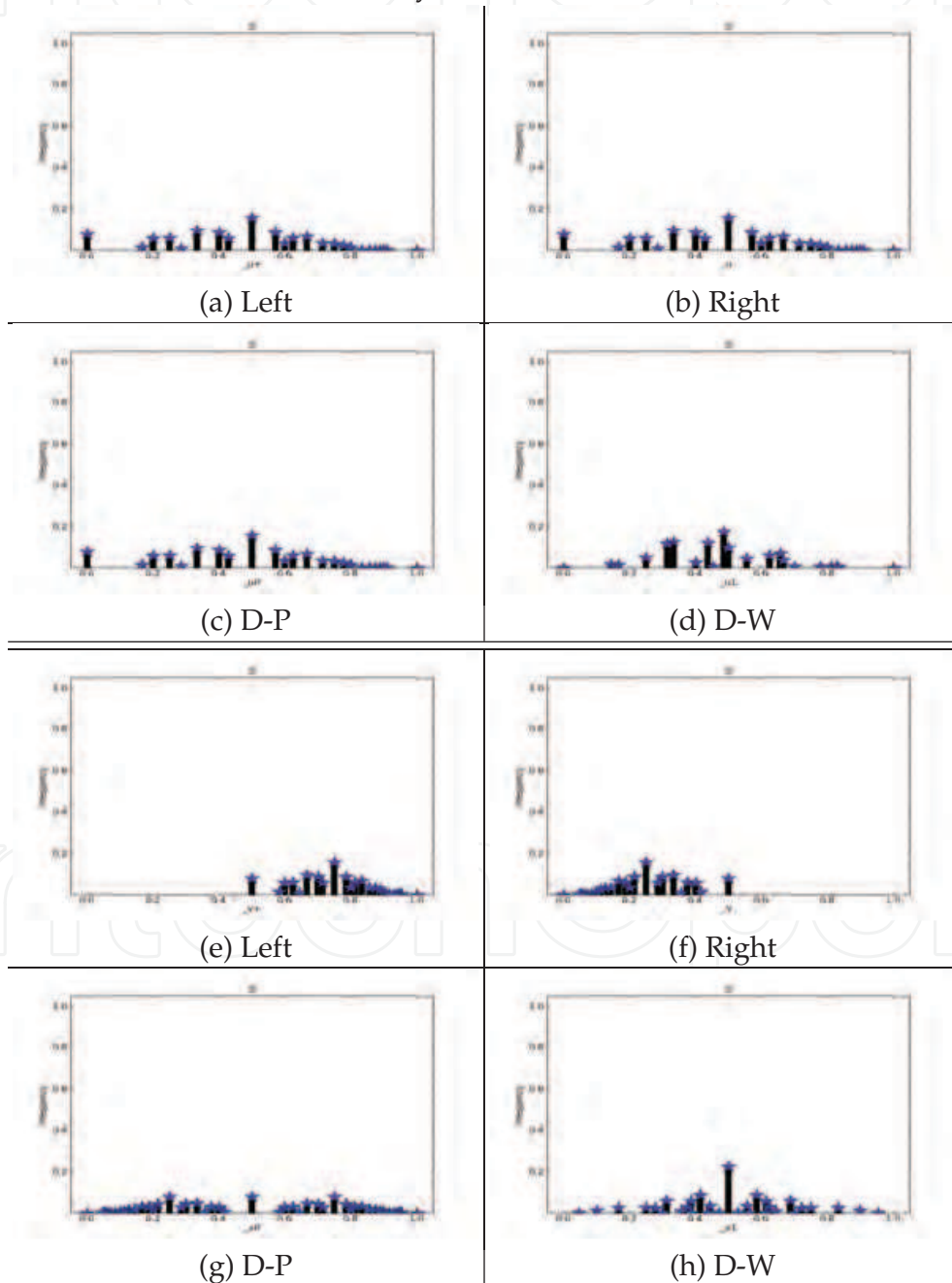
5.1 Statistical distributions

The simulation provides a series of output results. In this section, $N = \{12, 13\}, n = 2, \{J = 3, J_+ = 11, J_- = 2\}$ are selected. Corresponding to Left path (Left), Right path (Right), Double path for Particles (D-P) and Double path for Waves (D-W) under symmetry and anti-symmetry conditions respectively.

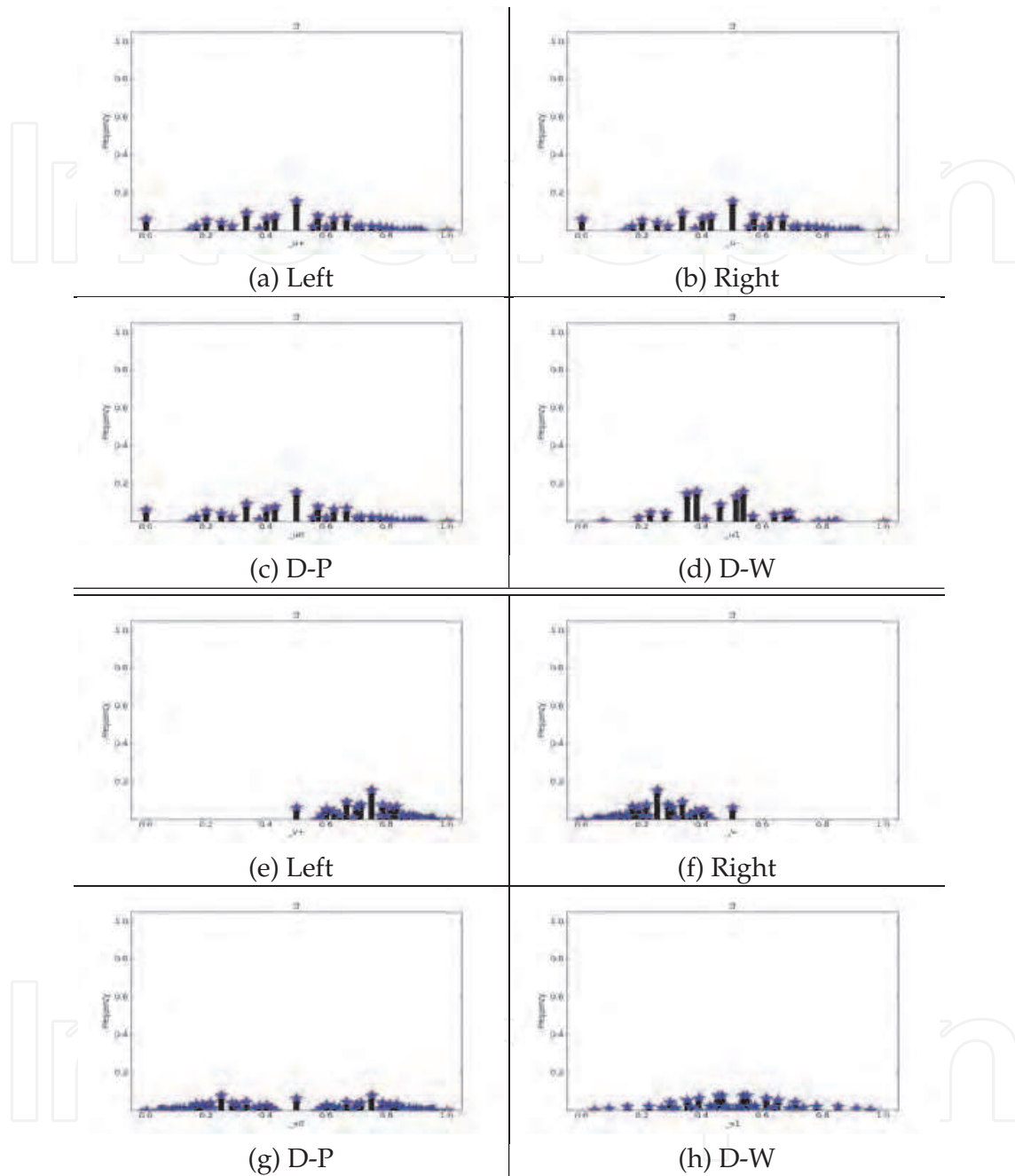
From a given function, a set of histograms can be generated as two groups of eight probability histograms. To show their refined properties, it is necessary to represent them in both odd and even numbers. A total of sixteen histograms are required. For convenience of comparison, sample cases are shown in Figures 3(I-III).

$P_H(\tilde{u}_+ J)$	$P_H(\tilde{u}_- J)$
(a) Left	(b) Right
$P_H(\tilde{u}_0 J)$	$P_H(\tilde{u}_1 J)$
(c) D-P	(d) D-W
$P_H(\tilde{v}_+ J)$	$P_H(\tilde{v}_- J)$
(e) Left	(f) Right
$P_H(\tilde{v}_0 J)$	$P_H(\tilde{v}_1 J)$
(g) D-P	(h) D-W

(I) Representative patterns of Histograms for function J (a-d) symmetric cases; (e-h) antisymmetric cases



(II) $N = \{12\}, J = 3$ Two groups of results in eight histograms



(III) $N = \{13\}, J = 3$ Two groups of results in eight histograms

Fig. 3. (I-III) $N = \{12, 13\}, J = 3$ Simulation results ; (I) Representative Patterns for $P_H(\tilde{u}_+|J) = P_H(\tilde{u}_-|J)$ and $P_H(\tilde{v}_+|J) = P_H(1 - \tilde{v}_-|J)$ conditions; (II) $N = \{12\}, J = 3$ Two groups of eight histograms on conditional probability; (III) $N = \{13\}, J = 3$ Two groups of eight histograms on conditional probability

Representation patterns are illustrated in Fig 3(I). Eight conditional probability histograms of $P_H(\tilde{u}_+|J) = P_H(\tilde{u}_+|J)$ are shown in Fig 3(II) for $N = 12$ to represent four symmetry groups and another eight conditional probability histograms are shown Fig 3(III) for $N = 13$ to represent four anti-symmetry groups respectively.

5.2 Global matrix representations

All possible 2^{2^n} functions are applied. It is convenient to arrange all the histograms generated into a matrix and a C code scheme of variant logic is applied to organize a set of 2^{2^n} histograms into a $2^{2^{n-1}} \times 2^{2^{n-1}}$ matrix.

Applying the C code configuration, any given signal of a function determines a matrix element to represent its histogram. There is one to one correspondence among different configurations.

Using this measurement mechanism, eight types of statistical histograms are systematically illustrated. Each element in the matrix is numbered to indicate its corresponding function and the relevant histogram is shown.

For $n = 2$ cases, sixteen matrices are shown in Figs 5-6 (a-h). Figs 5-6 (a-d) represent Symmetry groups and Figs 5-6 (e-h) represent Anti-symmetry groups. To show odd and even number configurations, Fig 5 (a-h) shows $N = 12$ cases and Fig 6 (a-h) shows $N = 13$ cases respectively.

6. Analysis of results

In the previous section, results of different statistical distributions and their global matrix representations were presented. In this section, plain language is used to explain what various visual effects might be illustrated and to discuss local and global arrangements.

6.1 Statistical distributions for a given function

It is necessary to analyze the differences among the various statistical distributions for a given function.

6.1.1 Symmetry groups for a function

For the selected function $J = 3$, four distributions in symmetry groups are shown in Fig 3 (a-d). (a) $P_H(\tilde{u}_+|J)$ for Left; (b) $P_H(\tilde{u}_-|J)$ for Right; (c) $P_H(\tilde{u}_0|J)$ for D-P; and (d) $P_H(\tilde{u}_1|J)$ for D-W respectively.

Under Symmetry conditions, $P_H(\tilde{u}_+|J) = P_H(\tilde{u}_-|J)$, both Left and Right distributions are the same. $P_H(\tilde{u}_0|J)$ generated with both paths open under asynchronous conditions simulates a D-P. Compared with distributions in (a-b), it is possible to identify the components from original inputs.

However, for $P_H(\tilde{u}_1|J)$ under synchronous conditions and with the same Left and Right input signals, the simulation shows a D-W exhibiting interferences among the output distributions that are significantly different from the original components.

6.1.2 Anti-symmetry groups for a function

Four distributions are shown in Fig 3 (e-h) as asymmetry groups. A pair of equations $P_H(\tilde{v}_+|J) = P_H(1 - \tilde{v}_-|J)$ shows that one distribution is a mirror image of the other. $P_H(\tilde{v}_+|J)$ distribution is shown in Fig 3 (e) for Left signals and $P_H(\tilde{v}_-|J)$ distribution is shown Fig 3 (f) for Right signals.

$P_H(\tilde{v}_0|J)$ is shown in Fig 3 (g) for both paths open under asynchronous conditions to simulate a D-P. Compared with (e-f) distributions, it is feasible to identify the same components from the original inputs.

However $P_H(\tilde{v}_1|J)$ is shown in Fig 3 (h) under synchronous condition with both path signals as inputs to simulate a D-W exhibiting interferences among the output distributions that are significantly different from the original components.

To differentiate between even and odd numbers, $N = 12$ cases are shown in Fig 3 (II, a-h) and $N = 13$ cases are shown in Fig 3 (III, a-h) respectively.

6.2 Global matrix representations

Sixteen matrices are represented in Fig 4-5 (a-h) with eight signals generating two sets of 16 groups for $N = \{12, 13\}$ respectively.

6.2.1 Symmetry cases

Matrices for the Left in Fig 4-5 (a) show elements in a column with the corresponding histogram showing polarized effects on the vertical.

Matrices for the Right in Fig 4-5 (b) show elements in a row with the corresponding histogram showing polarized effects on the horizontal.

Matrices for D-P in Fig 4-5 (c) provide asynchronous operations combined with both distributions from Fig 4-5 (a-b) to form a unified distribution. From each corresponding position, it is possible to identify each left and right component and the resulting shapes of the histogram.

Matrices for D-W in Fig 4-5 (d) provide synchronous operations combined with both distributions from Fig 4-5 (a-b) for each element.

Compared with Fig 4-5 (c) and Fig 4-5 (d) respectively, distributions in Fig 4-5 (d) are much simpler with two original distributions especially on the anti-diagonal positions: $J \in \{10, 12, 3, 5\}$. Only less than half the number of spectrum lines are identified.

6.2.2 Anti-symmetry cases

In a similar manner to the symmetry conditions, four anti-symmetry effects can be identified in Fig 4-5 (e-h). Matrices in Fig 4-5 (e) are Left operations for different functions; elements are polarized on the vertical and matrices in Fig 4-5 (f) are Right Operations; elements are polarized on the horizontal. Spectrum lines in Fig 4-5 (e) appear in the right half and spectrum lines in Fig 4-5 (f) appear in the Left half respectively.

Matrices for D-P in Fig 4-5 (g) show additional effects for each distribution according to the relevant position with components that can be identified as corresponding to identifiable inputs in many cases. Anti-symmetry signals are generated in merging conditions.

Matrices for D-W in Fig 4-5 (h) show different properties. In general, only one peak can be observed for each element especially for the $J \in \{10, 12, 3, 5\}$ condition. Spectra appear to be much simpler than the original distributions in Fig 4-5 (e-f), and significant interference properties are observed.

6.3 Four symmetry groups

Pairs of relationships can be checked on symmetry matrices in Figs 4-5 (a-d), four groups are identified.

6.3.1 Left: polarized vertical group

$\{P_H(\tilde{u}_+|J)\}$ elements in Figs 4-5 (a) show (only) four distinct distributions. Each column contains only one distribution. Sixteen elements in the matrix can be classified into four vertical classes: $\{0, 2, 8, 10\}$, $\{4, 6, 12, 14\}$, $\{1, 3, 9, 11\}$, $\{5, 7, 13, 15\}$ respectively. Four meta distributions are given as $\{10, 14, 11, 15\}$.

6.3.2 Right: polarized horizontal group

$\{P_H(\tilde{u}_-|J)\}$ elements in Figs 4-5 (b) show (a further) four distinct distributions. Each row contains only one distribution. Sixteen elements in the matrix can be classified into four horizontal classes: $\{0, 4, 1, 5\}$, $\{2, 6, 3, 7\}$, $\{8, 12, 9, 13\}$, $\{10, 14, 11, 15\}$ respectively. Four meta distributions are given as $\{0, 2, 8, 10\}$.

6.3.3 D-P: particle group

$\{P_H(\tilde{u}_0|J)\}$ elements in Figs 4-5 (c) illustrate symmetry properties. There are six pairs of symmetry elements: $\{8 : 14\}$, $\{2 : 11\}$, $\{0 : 15\}$, $\{6 : 9\}$, $\{4 : 13\}$, $\{1 : 7\}$. In addition, four elements on anti-diagonals provide different distributions: $\{10, 12, 3, 5\}$. Under this condition, ten classes of distributions are distinguished.

6.3.4 D-W: wave group

$\{P_H(\tilde{u}_1|J)\}$ elements in Figs 4-5 (d) illustrate symmetry properties. There are six pairs of symmetry elements: $\{8 : 14\}$, $\{2 : 11\}$, $\{0 : 15\}$, $\{6 : 9\}$, $\{4 : 13\}$, $\{1 : 7\}$. In addition, four elements on diagonal positions provide the same distribution: $\{0, 6, 9, 15\}$. Two elements on anti-diagonals: $\{12, 3\}$ have the same distribution in Fig 4 (d). Under this condition, nine or ten classes of different distributions can be identified for Fig 4 (d) and Fig 5 (d) respectively.

6.4 Four anti-symmetry groups

Figures 4-5 (e-h) represent anti-symmetry properties, four groups can be identified.

6.4.1 Left: polarized vertical group

$\{P_H(\tilde{\nu}_+|J)\}$ elements in Figs 4-5 (e) show that (only) four classes can be distinguished. Elements within these groups members are the same as for symmetry groups in Figs 4-5(a). Their distributions fall within the region $[0.5, 1]$.

6.4.2 Right: polarized horizontal group

$\{P_H(\tilde{\nu}_-|J)\}$ elements in Figs 4-5 (f) show that (only) four classes can be distinguished. Elements within these groups are the same as for symmetry groups in Figs 4-5 (b). Their distributions fall within the region $[0, 0.5]$.

6.4.3 D-P: particle group

$\{P_H(\tilde{\nu}_0|J)\}$ in Figs 4-5 (g) show six pairs of anti-symmetry distributions: $\{8 \uparrow 14\}, \{2 \uparrow 11\}, \{0 \uparrow 15\}, \{6 \uparrow 9\}, \{4 \uparrow 13\}, \{1 \uparrow 7\}$ four elements are distinguished on the anti-diagonals: $\{10, 12, 3, 5\}$. Under this condition, ten classes can be identified.

6.4.4 D-W: wave group

$\{P_H(\tilde{\nu}_1|J)\}$ in Figs 4-5 (h) show six pairs of anti-symmetry distributions: $\{8 \uparrow 14\}, \{2 \uparrow 11\}, \{0 \uparrow 15\}, \{6 \uparrow 9\}, \{4 \uparrow 13\}, \{1 \uparrow 7\}$ four pairs of symmetry elements: $\{3 : 5\}, \{10 : 12\}, \{2 : 4\}, \{11 : 13\}$ are distinguished. Under this condition, twelve classes can be identified.

6.5 Odd and even numbers

From a group viewpoint, only D-P and D-W need to be reviewed as different groups in symmetry conditions. Anti-symmetry conditions are unremarkable.

It is reasonable to suggest that anti-symmetry operations will be much easier to distinguish under experimental conditions, since sixteen groups in D-P conditions and twelve groups in D-W conditions will have significant differences. However, under the symmetry conditions (only) minor differences can be identified.

6.5.1 Single and double peaks

Single and Double peaks can be observed in Fig 4(5) (h): $\{3, 5\}$ for even and odd numbers respectively.

For two other members $\{10, 12\}$, (only) single pulse distributions are observed in Figs 4-5 (h) to show the strongest interference results.

6.6 Class numbers in different conditions

To summarize over the different classes, 16 matrices are shown in different numbers of identified classes as follows:

Class No.	Left	Right	D-P	D-W
SE	4	4	10	10
SO	4	4	10	10
AE	4	4	16	14
AO	4	4	16	14

where Left:Left Path, Right: Right Path, D-P: Double Path for Particles, D-W: Double Path for Waves; SE: Symmetry for Even number, SO: Symmetry for Odd number, AE: Anti-symmetry for Even number, AO: Anti-symmetry for Odd number.

6.7 Polarized effects and double path results

In order to contrast the different polarized conditions, it is convenient to compare distributions $\{P_H(\tilde{u}_+|J), P_H(\tilde{u}_-|J)\}$ and $\{P_H(\tilde{v}_+|J), P_H(\tilde{v}_-|J)\}$ arranged according to the corresponding polarized vertical and horizontal effects. This visual effect is similar to what might be found when using polarized filters in order to separate complex signals into two channels. Different distributions can be observed under synchronous and asynchronous conditions.

6.7.1 Particle distributions and representations

For all symmetry or non-symmetry cases under \oplus asynchronous addition operations, relevant values meet $0 \leq \tilde{u}_0, \tilde{v}_0, \tilde{u}_-, \tilde{v}_-, \tilde{u}_+, \tilde{v}_+ \leq 1$. Checking $\{P_H(\tilde{u}_0|J), P_H(\tilde{v}_0|J)\}$ series, $\{P_H(\tilde{u}_+|J), P_H(\tilde{u}_-|J)\}$ and $\{P_H(\tilde{v}_+|J), P_H(\tilde{v}_-|J)\}$ satisfy following equation.

$$\begin{cases} P_H(\tilde{u}_0|J) = \frac{P_H(\tilde{u}_-|J)+P_H(\tilde{u}_+|J)}{2} \\ P_H(\tilde{v}_0|J) = \frac{P_H(\tilde{v}_-|J)+P_H(\tilde{v}_+|J)}{2} \end{cases} \quad (16)$$

The equation is true for different values of N and n .

6.7.2 Wave distributions and representations

Interference properties are observed in $\{P_H(\tilde{u}_+|J) = P_H(\tilde{u}_-|J)\}$ conditions. Under + synchronous addition operations, relevant values meet $0 \leq \tilde{u}_1, \tilde{v}_1, \tilde{u}_-, \tilde{v}_-, \tilde{u}_+, \tilde{v}_+ \leq 1$. Checking $\{P_H(\tilde{u}_1|J), P_H(\tilde{v}_1|J)\}$ distributions and compared with $\{P_H(\tilde{u}_+|J), P_H(\tilde{u}_-|J)\}$ and $\{P_H(\tilde{v}_+|J), P_H(\tilde{v}_-|J)\}$, non-equations and equations are formulated as follows:

$$\begin{cases} P_H(\tilde{u}_1|J) \neq P_H(\tilde{u}_0|J) \\ P_H(\tilde{v}_1|J) \neq P_H(\tilde{v}_0|J) \end{cases} \quad (17)$$

Spectra in different cases illustrate wave interference properties. Single and double peaks are shown in interference patterns and these are similar to interference effects in classical double slit experiments.

6.7.3 Non-symmetry and non-anti-symmetry

However, for the $\{P_H(\tilde{u}_+|J) \neq P_H(\tilde{u}_-|J)\}$ non-symmetry cases, there are significant differences between $\{P_H(\tilde{u}_0|J), P_H(\tilde{v}_0|J)\}$ and $\{P_H(\tilde{u}_1|J), P_H(\tilde{v}_1|J)\}$. Such cases have interference patterns that exhibit greater symmetry than single path and particle distributions.

Four anti-diagonal positions are linked to symmetry and anti-symmetry pairs, twelve other pairs of functions belong to non-symmetry and non-anti-symmetry conditions. Their meta elements can be identified by the relevant variant expressions.

7. Core debated issues under variant construction

7.1 HUP environment

Under the variant construction, variant measurements can be organized into multiple sets of simultaneous measurements. Each element in a N bit vector provides only a small portion of information, collected measurements are independent of special positions. Under this condition, there is no essential HUP environment for the variant construction. 0-1 groups and their measurements are naturally parallel. They can be processed in simultaneous conditions. Considering these properties, such group measurements do not correspond with the requirements of Heisenberg single particle environments. Viewed as a whole, the system of the variant construction has discrete and separate properties that serve to facilitate complex local interactions for any selected group.

From a measurement viewpoint, the parallel parameters of the variant measurements enable them to exist in different interactive models simultaneously. This set of simultaneous properties exhibits significant differences between the original wave functions and the variant construction.

7.2 Weakness of BCP

The main weakness of the BCP lies deep in the very logic on which it is founded. In his approach to QM, Bohr applied then extant classical principles of logic using static YES/NO approaches to dynamic particle and wave measurements. However, the complex nature of QM phenomena means that such a classical logic framework cannot fully support this quaternion organization or fully model the dynamic systems involved. This is the main reason why the BCP requires the application of exclusive properties to pairs of opposites.

The variant construction provides quaternion measurement groups. This property naturally supports QM-like structures. Useful configurations can be chosen for further development.

The main experimental evidence following Bohr in rejecting particle models are sets of wave interference distributions generated in long duration and very low intensity single photon experiments. These experiments show intrinsic wave interference patterns under many environments. Understandably, such data have long been held to be strongly indicative of wave properties within even single quanta. Consequently, it has been deemed natural and necessary to apply wave descriptions and analysis tools in the search for QM solutions.

However, evidence residing within the main visual distributions of this chapter, serves to show that statistical distributions under a conditional probability environment naturally link to intrinsic wave properties in the majority of situations. Nearly all interesting distributions show obvious wave properties. Notably, such intrinsic wave distributions may be sufficient to allow a satisfactory alternative explanation of experimental results generated in long duration and very low intensity single photon experiments.

7.3 The BCP for a special subset of QM

We may deduce that there is (only) a special subset of QM for which the BCP is satisfied. Under the variant construction there are six distinct logical configurations that can be used to support 0-1 vectors. Of these six, Bohr’s approach is suitable for only the two schemes of pure static YES or NO. Meanwhile, the other four variant, invariant and mixed configurations lie outside the BCP framework. From this viewpoint, Bohr offers insight into important special circumstances of QM rather than provides an all embracing general solution.

Bohr’s QM construction is complete and useful in many theoretical and practical environments for static and static-like systems. However, the variant construction provides a more powerful and general mechanism to handle different dynamic systems with variant and invariant properties.

7.4 The EPR contribution on variant construction

From EPR proposed experiments and other theoretical considerations, Einstein demonstrated a depth of understanding of weakness inherent in the foundations of the QM approach. He clearly identified two operators with non-communication properties that failed to support simultaneous operations and recognized that this type of mechanism was still not explained in the Copenhagen interpretation.

Using the variant construction, EPR devices have the following correspondence:

$$\begin{cases} S_1 & \rightarrow \{u_\beta, v_\beta, \tilde{u}_\beta, \tilde{v}_\beta \dots\}; \\ S_2 & \rightarrow \{u_\beta, v_\beta, \tilde{u}_\beta, \tilde{v}_\beta \dots\}; \\ IM(S_1, S_2) & \rightarrow \{M(u_1), M(v_1), M(\tilde{u}_1), M(\tilde{v}_1) \dots\}; \\ SM(S_1, S_2) & \rightarrow \{M(u_0), M(v_0), M(\tilde{u}_0), M(\tilde{v}_0) \dots\}. \end{cases} \quad (18)$$

$$\begin{cases} \langle S_1, S_2, IM(S_1, S_2), SM(S_1, S_2) \rangle \rightarrow \\ \langle \{u_\beta, v_\beta, \tilde{u}_\beta, \tilde{v}_\beta \dots\}, \{u_\beta, v_\beta, \tilde{u}_\beta, \tilde{v}_\beta \dots\}, \\ \{M(u_1), M(v_1), M(\tilde{u}_1), M(\tilde{v}_1) \dots\}, \\ \{M(u_0), M(v_0), M(\tilde{u}_0), M(\tilde{v}_0) \dots\} \rangle \end{cases} \quad (19)$$

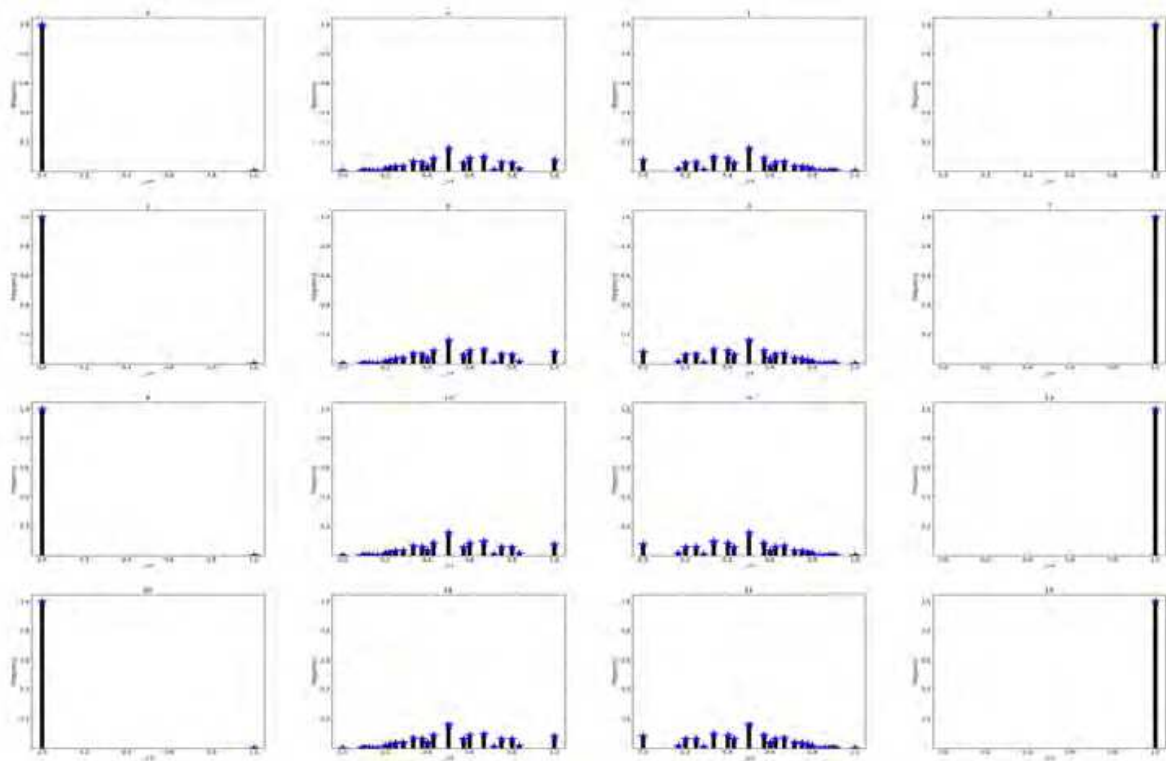
From this correspondence, many possible configurations of combinations and their subsets are available for future theoretical and experimental exploration.

Using the variant construction, rich configurations can be expressed. From such mapping, it can be seen to be nothing less than astounding that such meta constructions were identified by Einstein as far back as 1935.

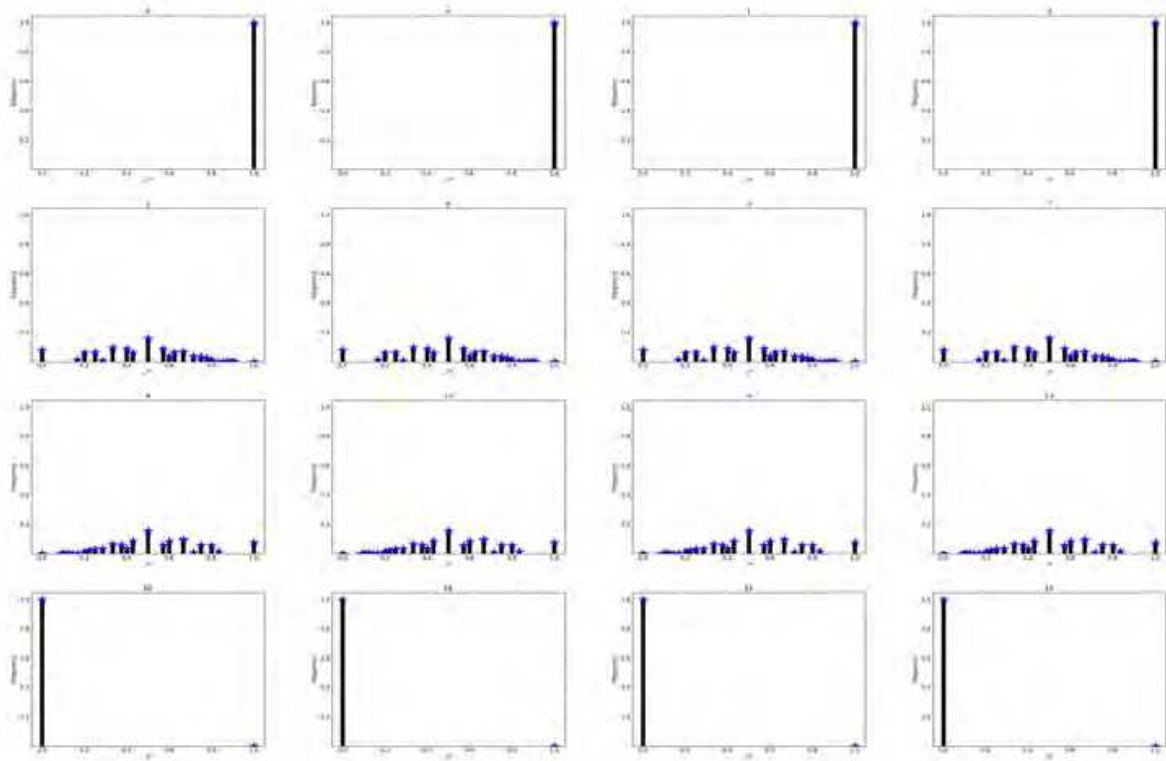
7.5 Afshar’s experiments on variant construction

Afshar’s experiments apply anti-symmetry signals making the following correspondence:

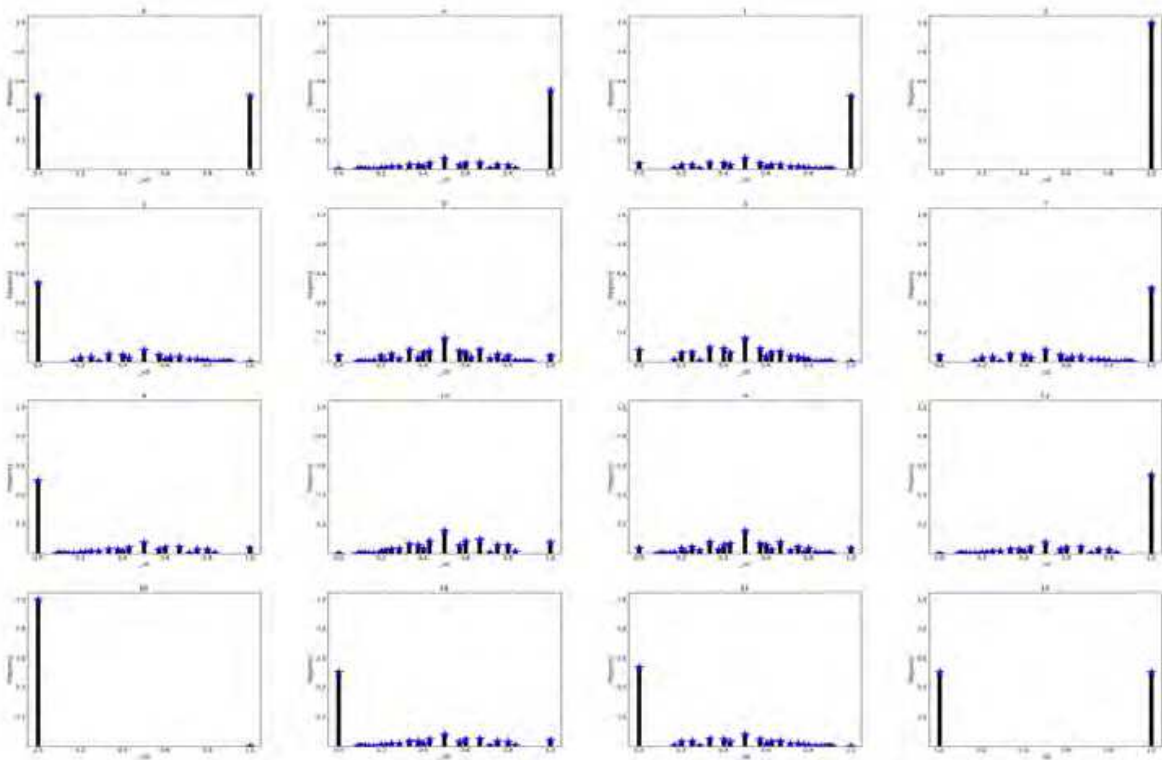
$$\begin{cases} \psi_1 & \rightarrow \{v_+\}; \\ \psi_2 & \rightarrow \{v_1\}; \\ \sigma_1 & \rightarrow \{P_H(v_1|J)\}; \\ \sigma_2 & \rightarrow \{P_H(v_0|J)\}. \end{cases} \quad (20)$$



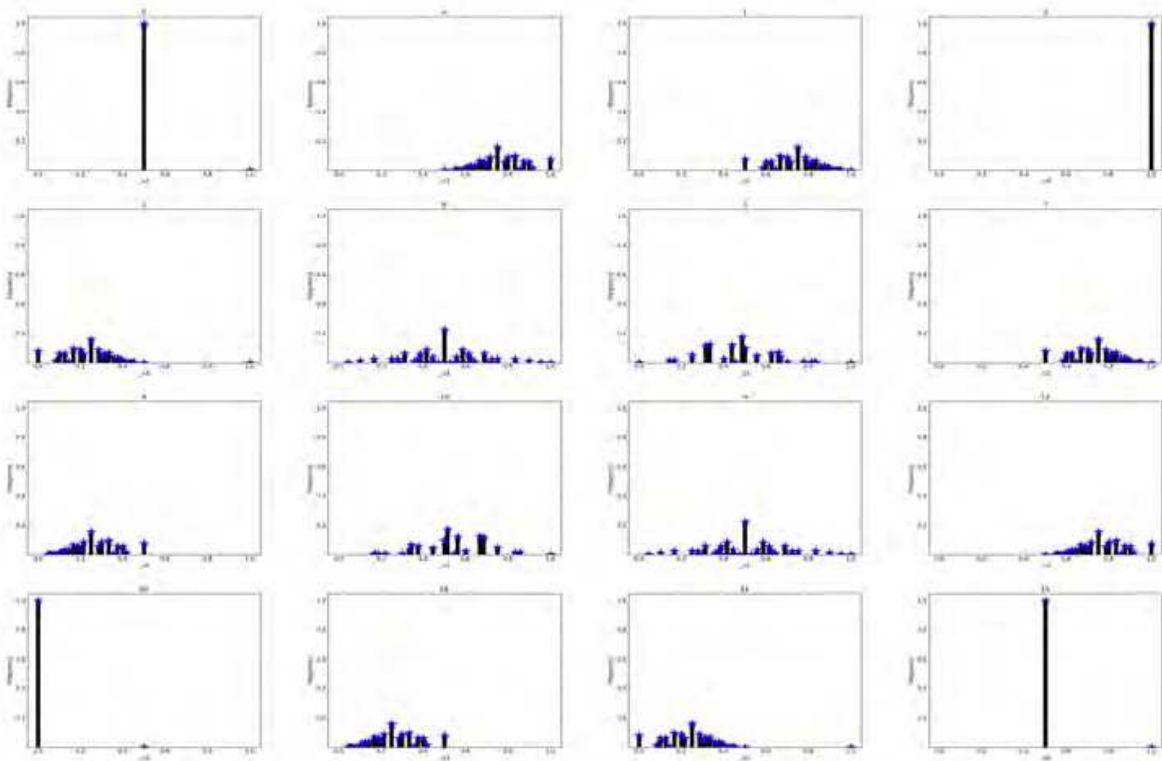
(a) Left



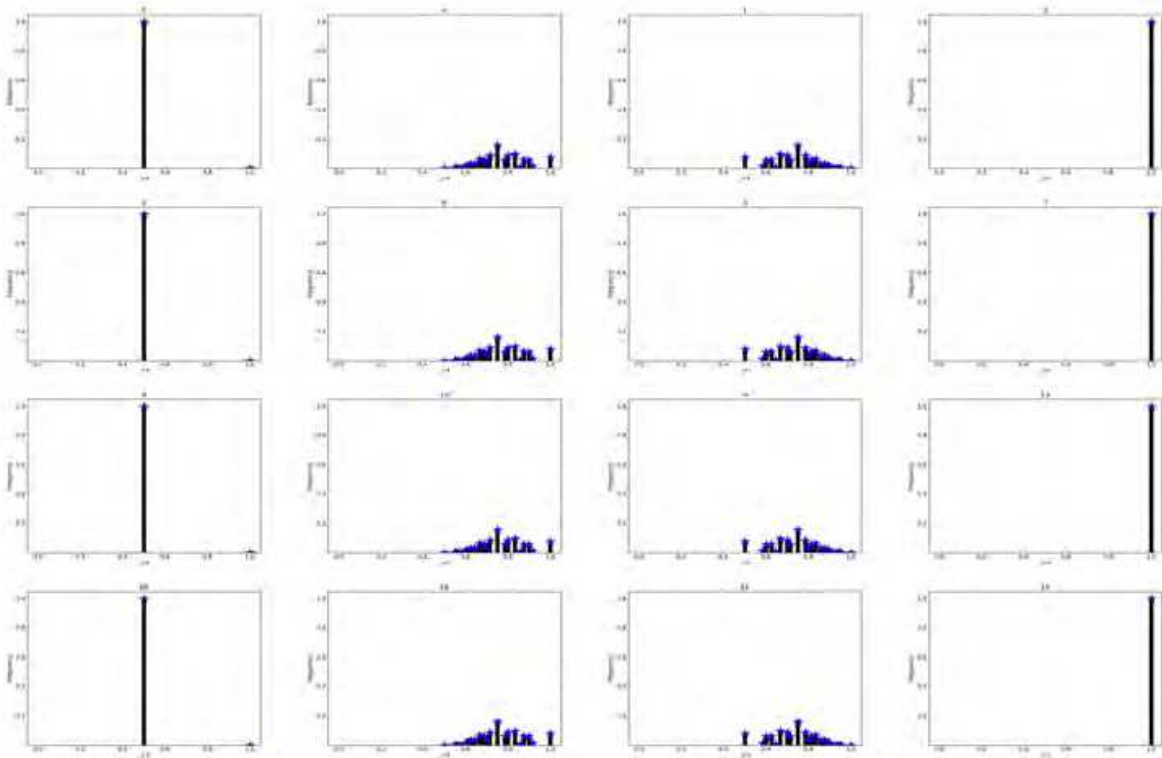
(b) Right



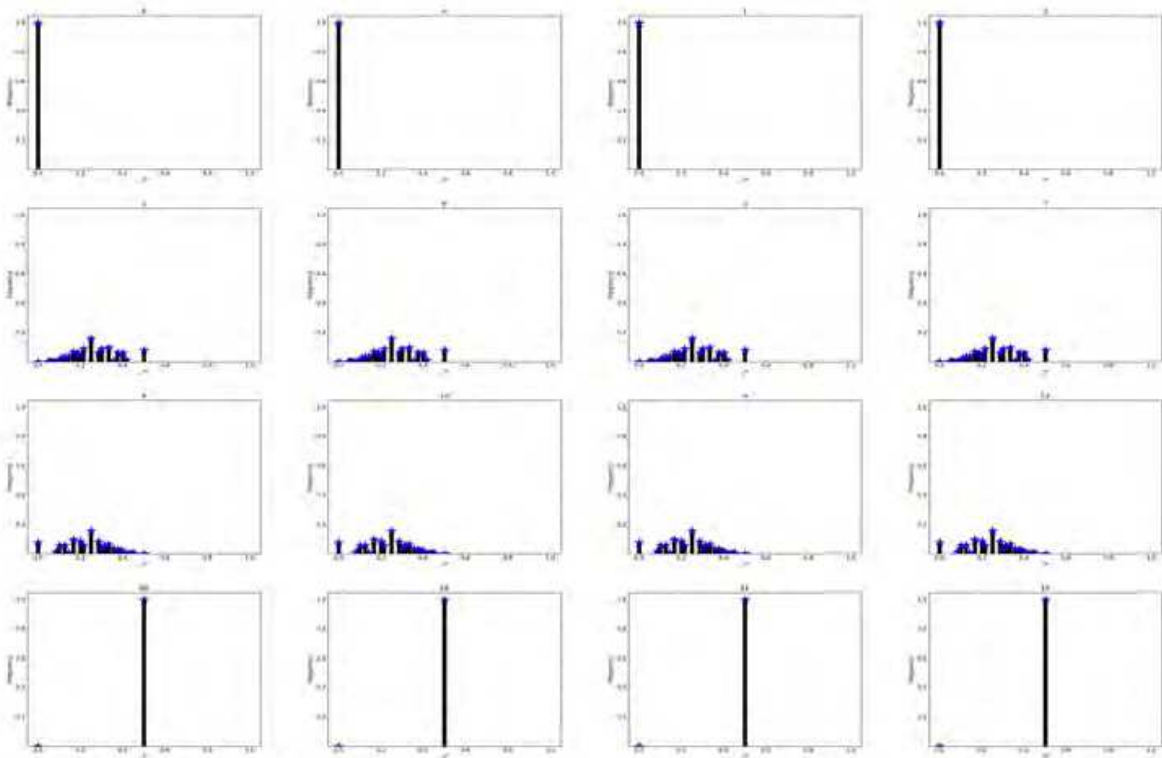
(c) D-P



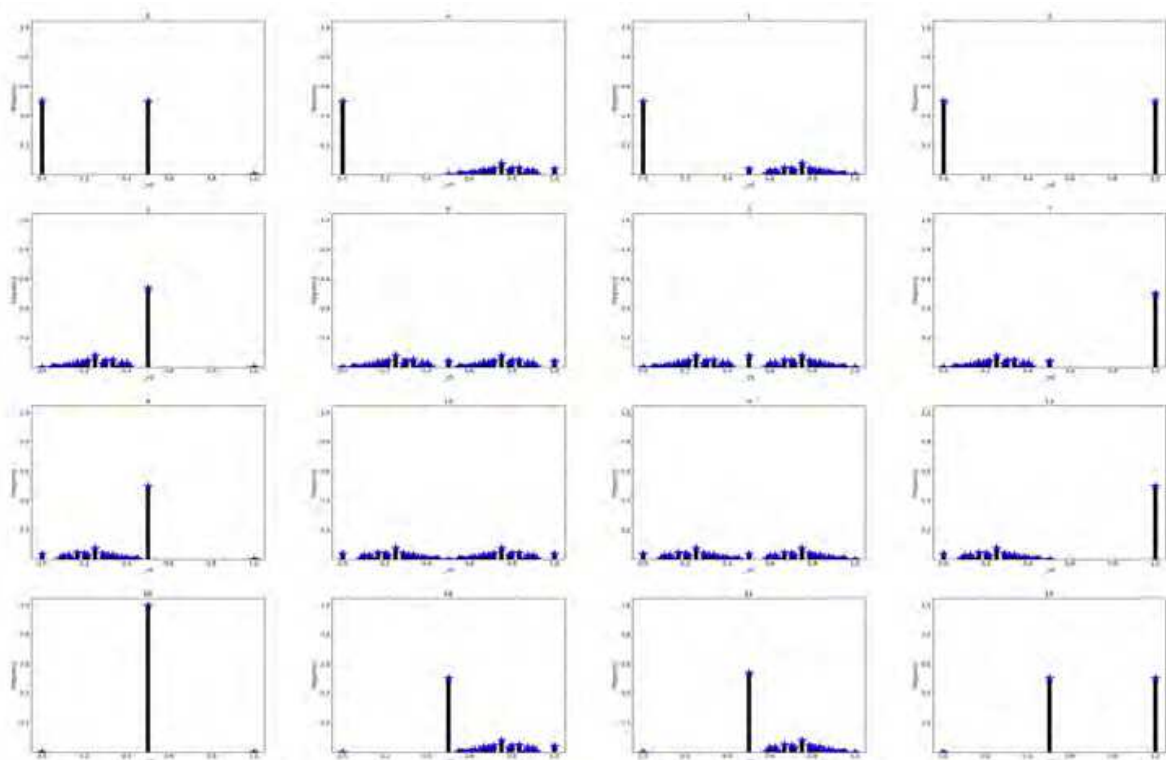
(d) D-W



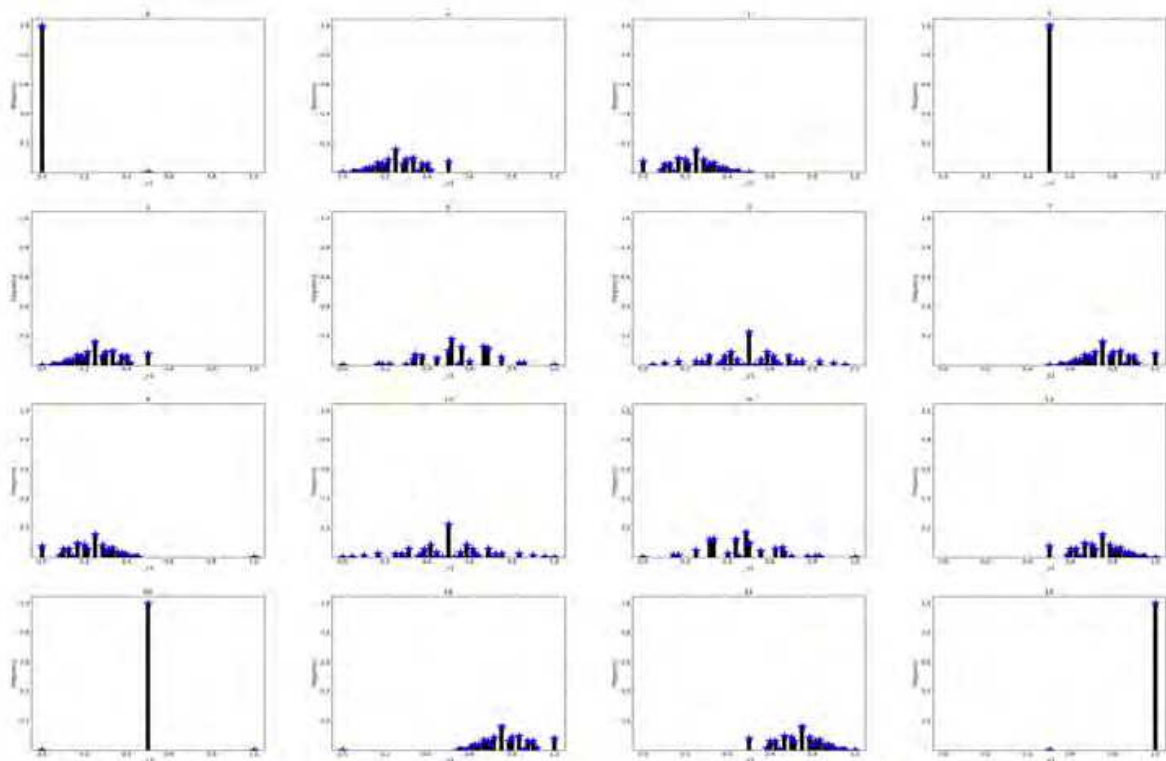
(e) Left



(f) Right

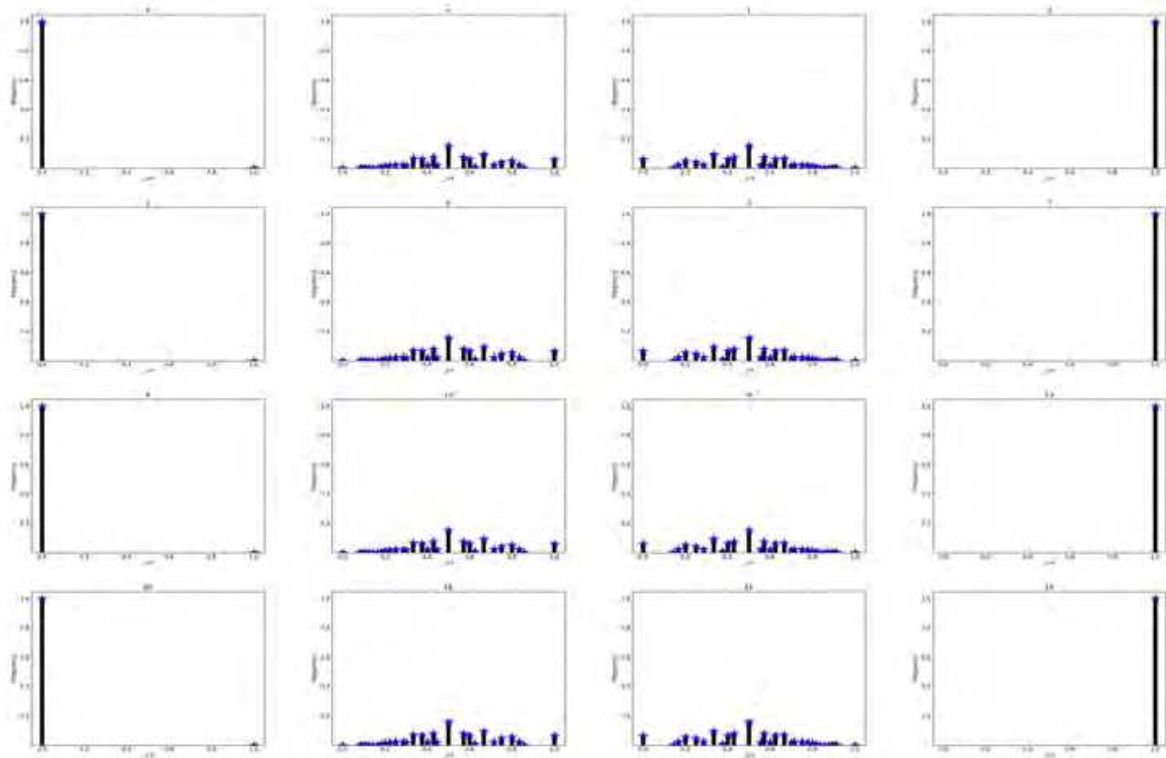


(g) D-P

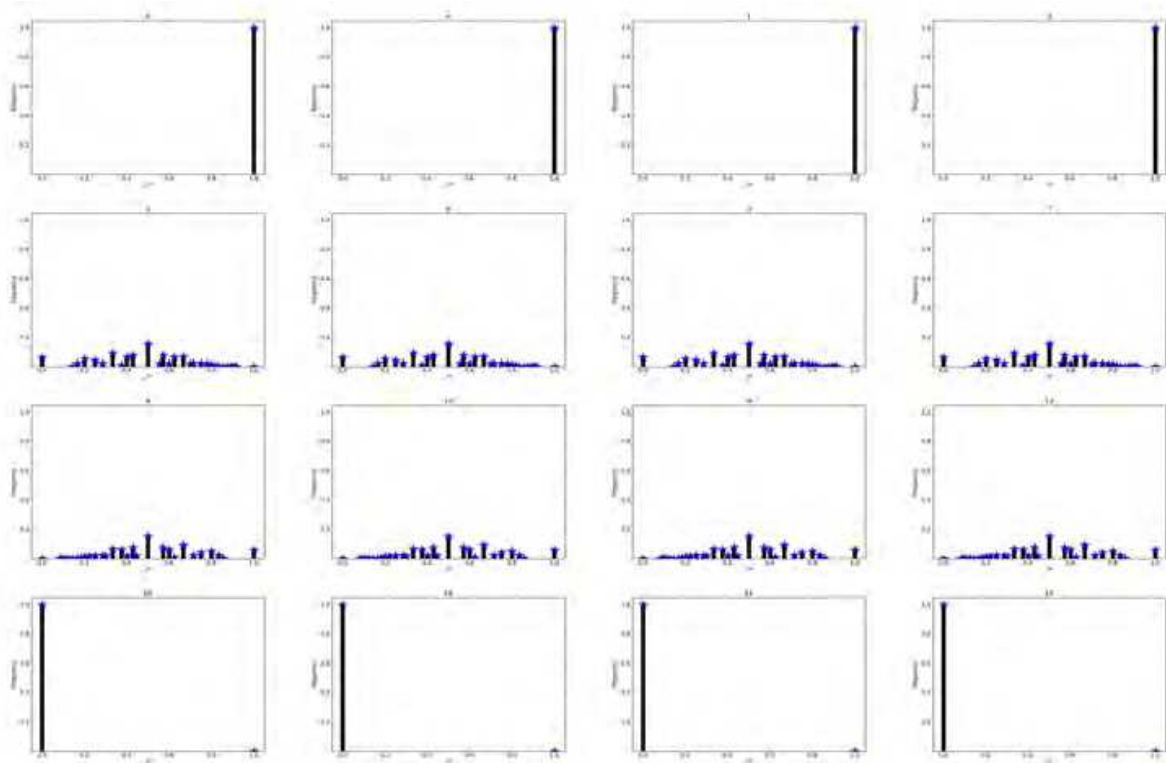


(h) D-W

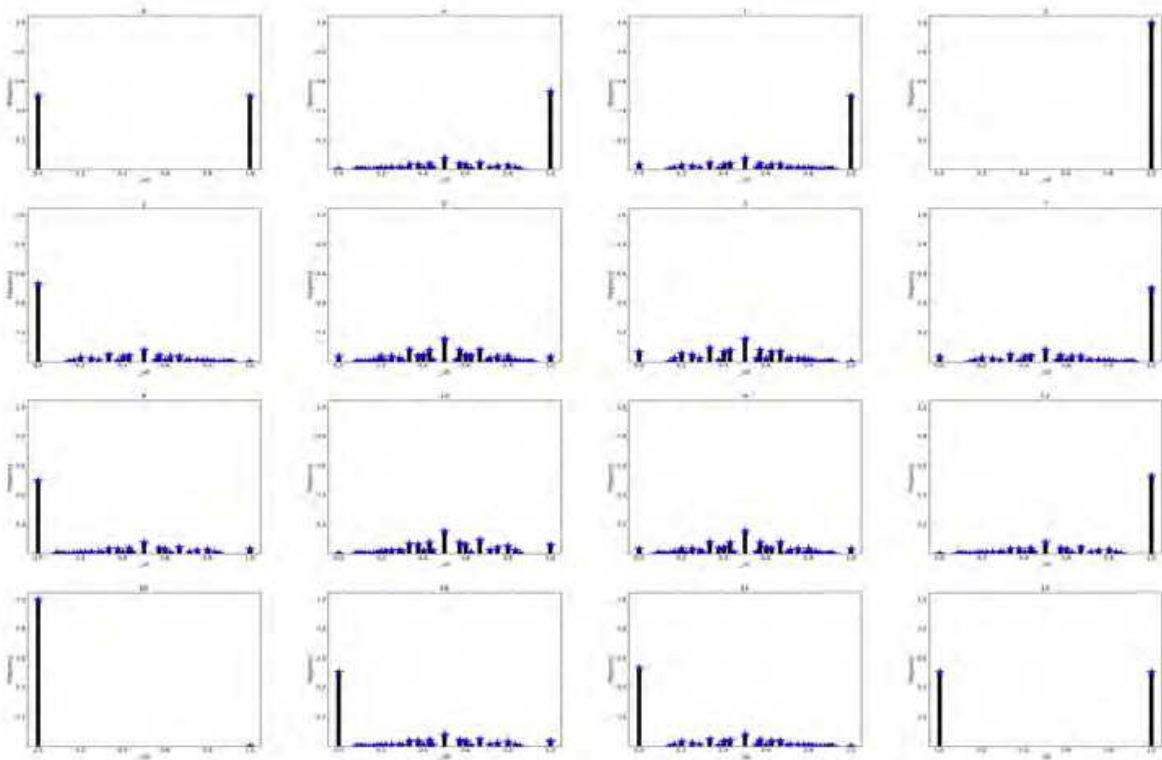
Fig. 4. (a-h) Even number groups: $N = \{12\}$, $f \in B_2^4$ Eight Matrices of Global Matrix Representations. (a) Left; (b) Right; (c) D-P; (d)D-W in symmetry conditions; (e) Left; (f) Right; (g) D-P; (h)D-W in anti-symmetry conditions.



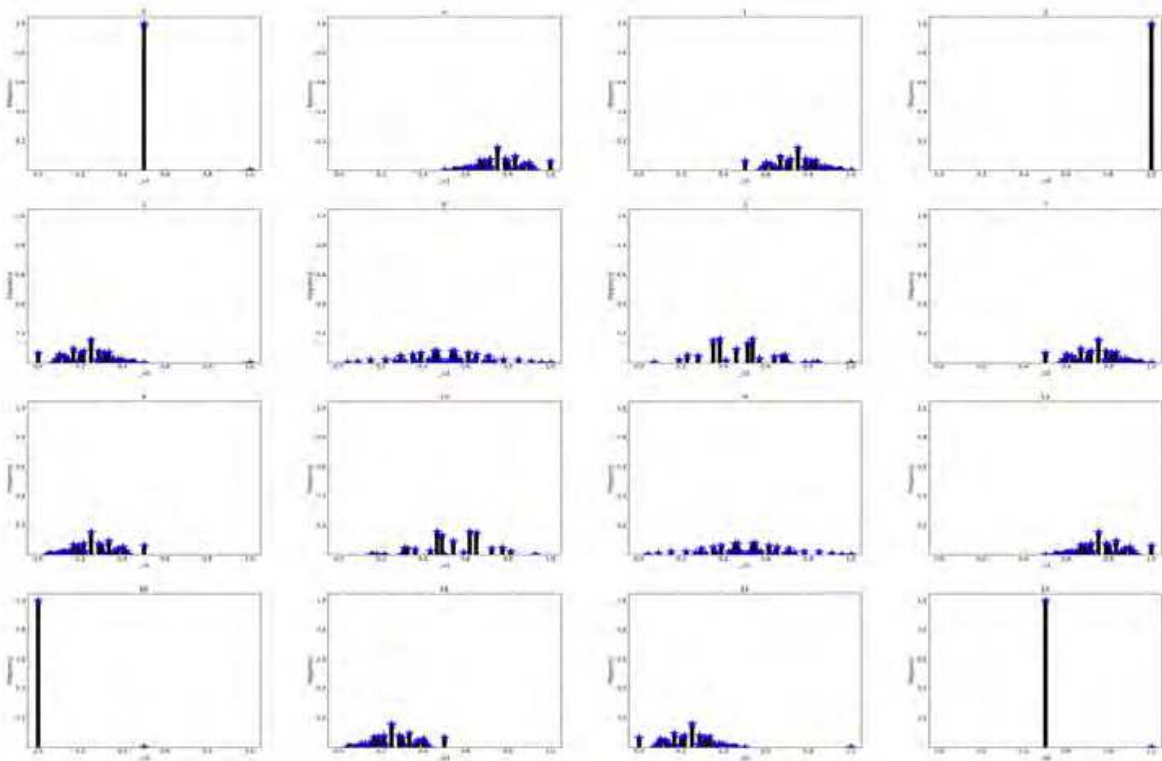
(a) Left



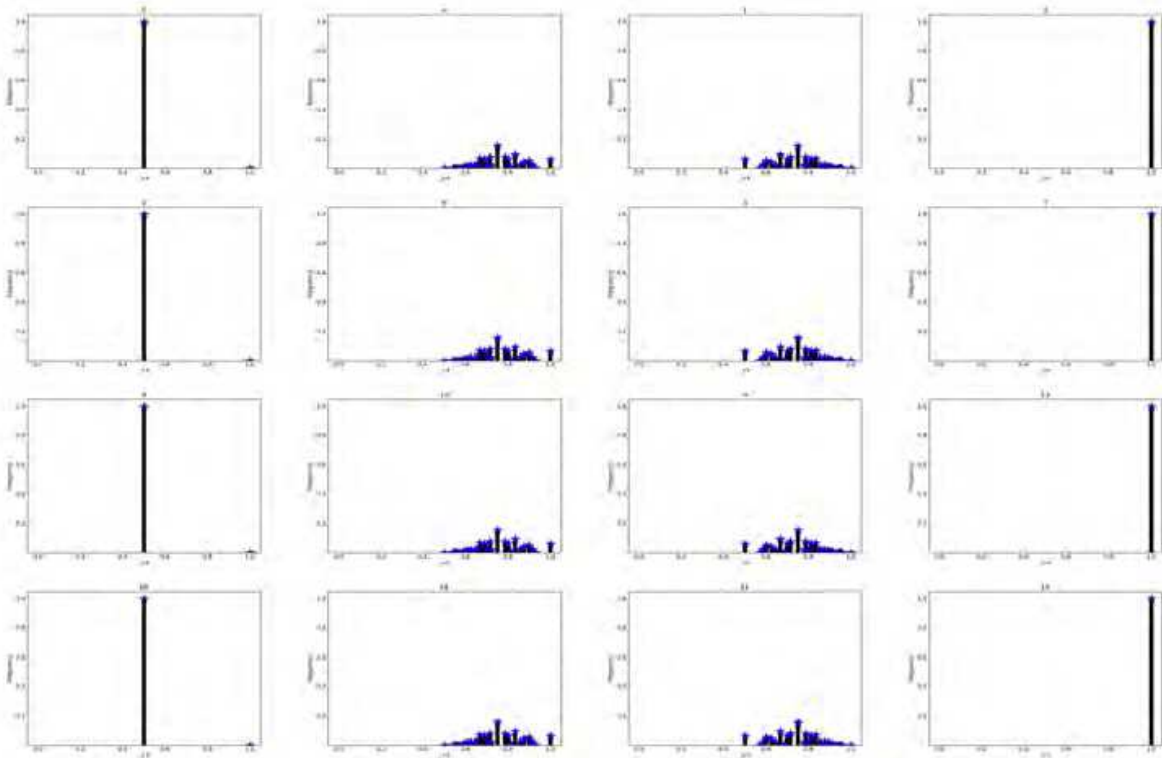
(b) Right



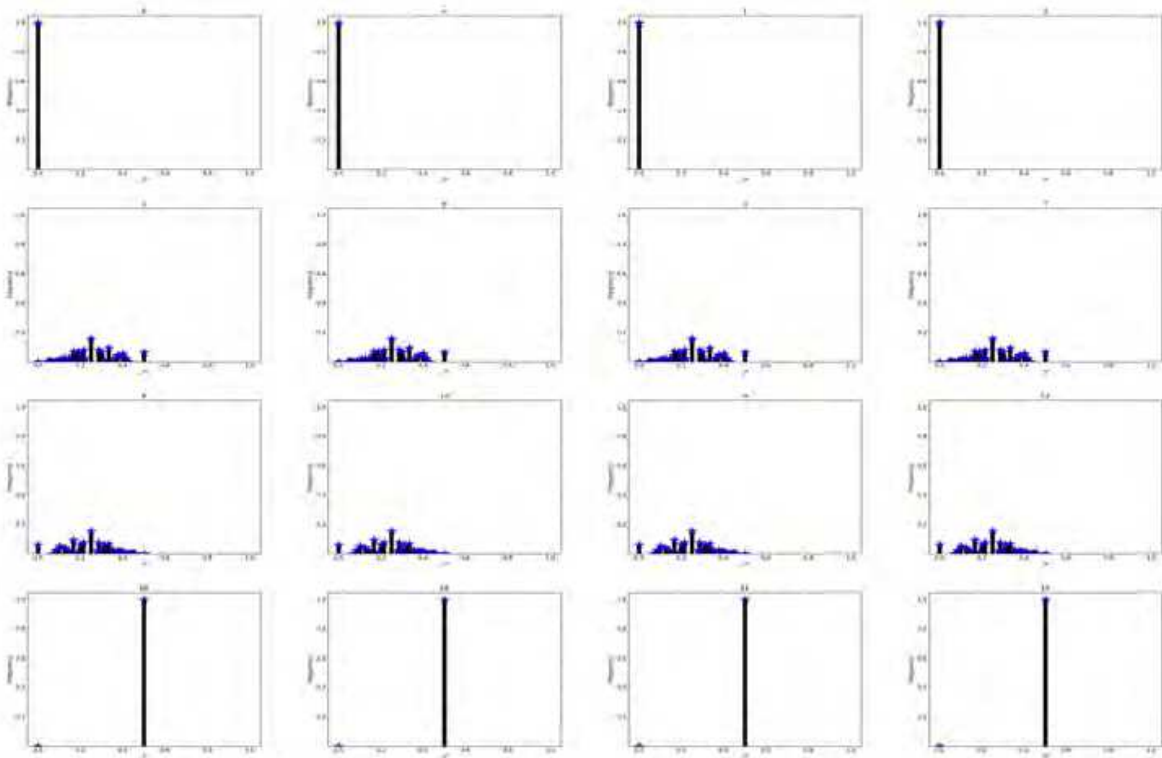
(c) D-P



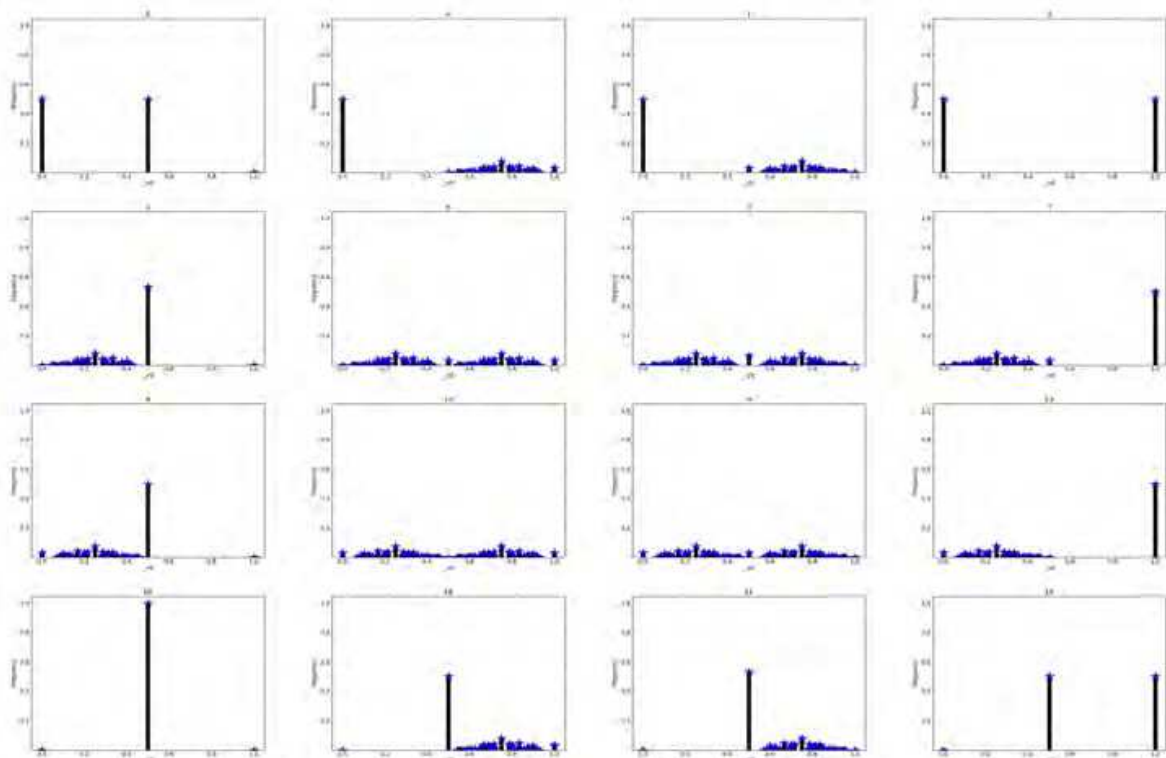
(d) D-W



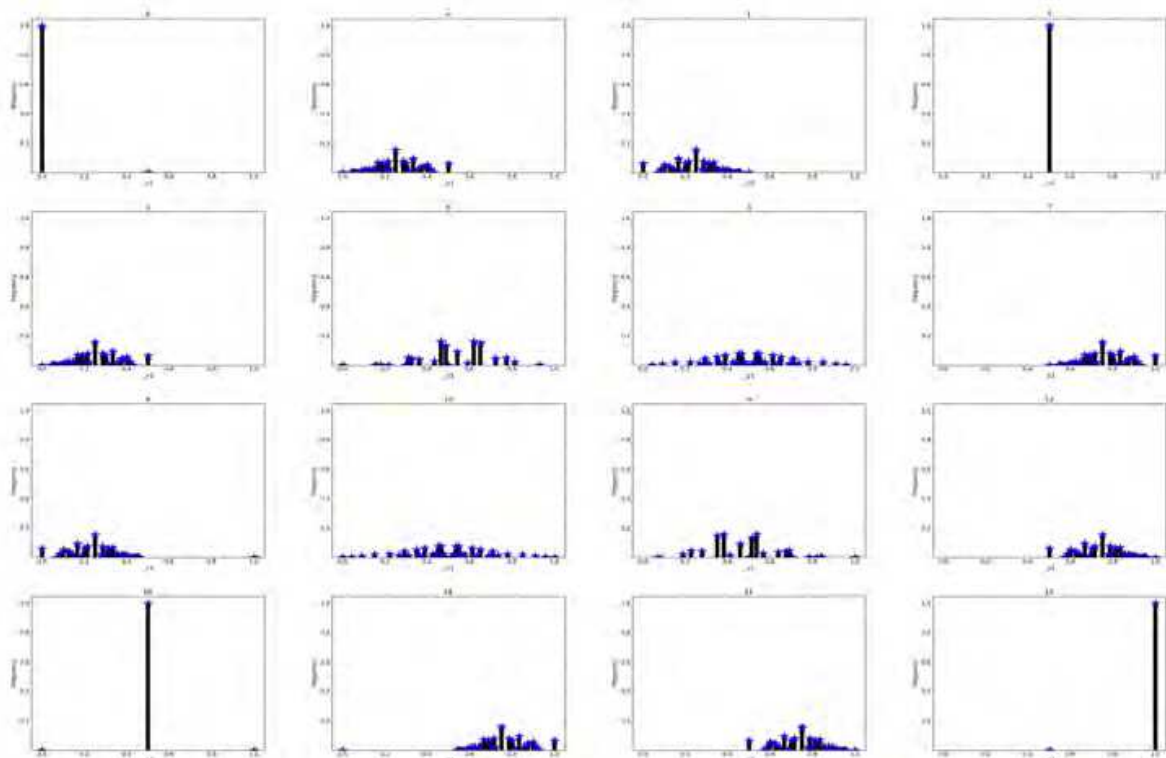
(e) Left



(f) Right



(g) D-P



(h) D-W

Fig. 5. (a-h) Odd number groups: $N = \{13\}, f \in B_2^4$ Eight Matrices of Global Matrix Representations. (a) Left; (b) Right; (c) D-P; (d) D-W in symmetry conditions; (e) Left; (f) Right; (g) D-P; (h) D-W in anti-symmetry conditions.

Using quaternion structures,

$$\{ \langle \psi_1, \psi_2, \sigma_1, \sigma_2 \rangle \rightarrow \langle \{v_+\}, \{v_1\}, \{P_H(v_1|J)\}, \{P_H(v_0|J)\} \rangle. \quad (21)$$

All Afshar's experiments are a special case of the EPR model.

8. Main results

Presented as predictions and conjectures:

8.1 Predictions

Commensurate with the chapter of local interactive measurements, similar predictions can be described under conditional probability conditions:

Prediction 1: Left distributions have relationships showing polarized vertical behaviors with intrinsic wave properties on conditional environments.

Prediction 2: Right distributions have relationships showing polarized horizontal behaviors with intrinsic wave properties on conditional environments.

Prediction 3: D-P distributions have relationships showing classical particle statistical behaviors with intrinsic wave properties on conditional environments.

Prediction 4: D-W distributions have relationships showing wave interference statistical behaviors with strong wave properties on conditional environments.

Prediction 5: Afshar's experiments are a special case of the EPR model in real photon experimental environments.

Prediction 6: Distributions on conditional environments provide essential evidence to support a series of experimental results on quanta self-interference properties.

8.2 Conjectures

Presented in relation to milestones in the historical debate underpinning the foundations of QM:

Conjecture 1. Einstein may be declared the winner in the Bohr-Einstein debates on QM.

Conjecture 2. EPR construction is a super-powerful model to support different measurements and simulations of quantum behaviors.

Conjecture 3. The variant construction provides a logical measurement based foundation to support the simulation and visualization of quantum behaviors.

Conjecture 4. The next generation of fundamental development in QM will grow out of further theoretical and experimental exploration based on variant construction.

9. Conclusion

Long held views on the wave/particle enigma, especially those investigated through single photon experiments may be founded on a special case rather than a general explanation.

Further insight may be found working from conditional probability measurements to global matrix representation on the variant construction.

Applying conditional probability models on interactive measurements and relevant statistical processes, two groups of parameters $\{\tilde{u}_\beta, \tilde{v}_\beta\}$ describe left path, right path, D-P and D-W conditions with distinguishing symmetry and anti-symmetry properties. $\{P_H(\tilde{u}_\beta|J), P_H(\tilde{v}_\beta|J)\}$ provide eight groups of distributions under symmetry and anti-symmetry forms. In addition, $\{M(\tilde{u}_\beta), M(\tilde{v}_\beta)\}$ provide eight matrices to illustrate global behaviors under conditional environments.

The complexity of n -variable function space has a size of 2^{2^n} and exhaustive vector space has 2^N . Overall simulation complexity is determined by $O(2^{2^n} \times 2^N)$ as ultra exponent productions. How to overcome the limitations imposed by such complexity and how best to compare and contrast such simulations with real world experimentation will be key issues in future work.

Six predictions and four conjectures are offered for testing by further theoretical and experimental work.

10. Acknowledgements

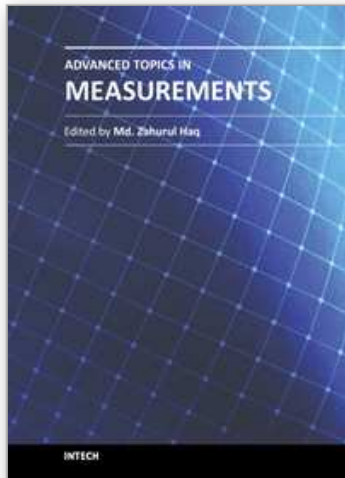
Thanks to Colin W. Campbell for help with the English edition, to The School of Software Engineering, Yunnan University and The Key Laboratory of Yunnan Software Engineering for financial supports to the Information Security research projects (2010EI02, 2010KS06) and sub-CDIO project.

11. References

- Afshar, S. (2005). Violation of the principle of complementarity, and its implications, *Proc. SPIE* 5866. 229-244.
- Afshar, S. (2006). Violation of bohr's complementarity: One slit or both?, *AIP Conf. Proc.* 810. 294-299.
- Afshar, S., Flores, E., McDonald, K. & Knoesel, E. (2007). Paradox in wave particle duality, *Found. Phys.* 37. 295-305.
- Ash, R. B. & Doléans-Dade, C. A. (2000). *Probability & Measure Theory*, Elsevier.
- Aspect, A. (2007). To be or not to be local, *Nature* 446. 866-867.
- Aspect, A., Grangier, P. & Roger, G. (1982). Experimental realization of einstein -podolsky -rosen-bohm gedankenexperiment: A new violation of bell's inequalities, *Phys. Rev. Lett.* 49. 91-94.
- Barrow, J. D., Davies, P. C. W. & Charles L. Harper, J. E. (2004). *SCIENCE AND ULTIMATE REALITY: Quantum Theory, Cosmology and Complexity*, Cambridge University Press.
- Bell, J. S. (1964). On the einstein-podolsky-rosen paradox, *Physics* 1. 195-200.
- Bohr, N. (1935). Can quantum-mechanical description of physical reality be considered complete?, *Physical Review* 48. 696-702.
- Bohr, N. (1949). *Discussion with Einstein on Epistemological Problems in Atomic Physics*, Evanston. 200-241.
- Bohr, N. (1958). *Atomic Physics and Human Knowledge*, Wiley.
- Bolles, E. (2004). *Einstein Defiant*, Joseph Henry Press.
- Born, M. (1971). *The Born Einstein Letters*, Walker and Company.

- Clauser, J., Horne, N., Shimony, A. & Holt, R. (1969). Proposed experiment to test local hidden-variable theories, *PRL* 23. 880-884.
- Durret, R. (2005). *Probability: Theory and Examples*, Thomson.
- Einstein, A., Podolsky, B. & Rosen, N. (1935). Can quantum-mechanical description of physical reality be considered complete?, *Physical Review* 47. 770-780.
- Feynman, R., Leighton, R. & Sands, M. (1965,1989). *The Feynman Lectures on Physics*, Vol. 3, Addison-Wesley, Reading, Mass.
- Hawking, S. & Mlodinow, L. (2010). *The Grand Design*, Bantam Books.
- Heisenberg, W. (1930). *The Physical Principles of Quantum Theory*, Uni. Chicago Press.
- Jammer, M. (1974). *The Philosophy of Quantum Mechanics*, Wiley-Interscience Publication.
- Penrose, R. (2004). *The Road to Reality*, Vintage Books, London.
- Valiant, L. (1975). Parallelism in comparison problems, *SIAM J. Comput.* 4(3). 348-355.
- Zheng, J. (2011). Synchronous properties in quantum interferences, *Journal of Computations & Modelling, International Scientific Press* 1(1). 73-90.
URL: http://www.sciencpress.com/upload/JCM/Vol%201_1_6.pdf
- Zheng, J. & Zheng, C. (2010). A framework to express variant and invariant functional spaces for binary logic, *Frontiers of Electrical and Electronic Engineering in China, Higher Education Press and Springer* 5(2): 163-172.
URL: <http://www.springerlink.com/content/91474403127n446u/>
- Zheng, J. & Zheng, C. (2011a). Variant measures and visualized statistical distributions, *Acta Photonica Sinica, Science Press* 40(9). 1397-1404.
URL: <http://www.photon.ac.cn/CN/article/downloadArticleFile.do?attachType=PDF&id=15668>
- Zheng, J. & Zheng, C. (2011b). Variant simulation system using quaternion structures, *Journal of Modern Optics, Taylor & Francis Group*. iFirst 1-9.
URL: <http://www.tandfonline.com/doi/abs/10.1080/09500340.2011.636152>
- Zheng, J., Zheng, C. & Kunii, T. (2011). A framework of variant-logic construction for cellular automata, *Cellular Automata - Innovative Modelling for Science and Engineering edited Dr. Alejandro Salcido, InTech Press*. 325-352, ISBN 978-953-307-172-5.
URL: <http://www.intechopen.com/articles/show/title/a-framework-of-variant-logic-construction-for-cellular-automata>

IntechOpen



Advanced Topics in Measurements

Edited by Prof. Zahurul Haq

ISBN 978-953-51-0128-4

Hard cover, 400 pages

Publisher InTech

Published online 07, March, 2012

Published in print edition March, 2012

Measurement is a multidisciplinary experimental science. Measurement systems synergistically blend science, engineering and statistical methods to provide fundamental data for research, design and development, control of processes and operations, and facilitate safe and economic performance of systems. In recent years, measuring techniques have expanded rapidly and gained maturity, through extensive research activities and hardware advancements. With individual chapters authored by eminent professionals in their respective topics, *Advanced Topics in Measurements* attempts to provide a comprehensive presentation and in-depth guidance on some of the key applied and advanced topics in measurements for scientists, engineers and educators.

How to reference

In order to correctly reference this scholarly work, feel free to copy and paste the following:

Jeffrey Zheng, Christian Zheng and T.L. Kunii (2012). From Conditional Probability Measurements to Global Matrix Representations on Variant Construction – A Particle Model of Intrinsic Quantum Waves for Double Path Experiments, *Advanced Topics in Measurements*, Prof. Zahurul Haq (Ed.), ISBN: 978-953-51-0128-4, InTech, Available from: <http://www.intechopen.com/books/advanced-topics-in-measurements/from-conditional-probability-measurements-to-global-matrix-representations-on-variant-construction>

INTECH
open science | open minds

InTech Europe

University Campus STeP Ri
Slavka Krautzeka 83/A
51000 Rijeka, Croatia
Phone: +385 (51) 770 447
Fax: +385 (51) 686 166
www.intechopen.com

InTech China

Unit 405, Office Block, Hotel Equatorial Shanghai
No.65, Yan An Road (West), Shanghai, 200040, China
中国上海市延安西路65号上海国际贵都大饭店办公楼405单元
Phone: +86-21-62489820
Fax: +86-21-62489821

© 2012 The Author(s). Licensee IntechOpen. This is an open access article distributed under the terms of the [Creative Commons Attribution 3.0 License](#), which permits unrestricted use, distribution, and reproduction in any medium, provided the original work is properly cited.

IntechOpen

IntechOpen